

Towards *ab initio* simulation of quantum plasmas and warm dense matter

Michael Bonitz, Simon Groth, Tobias Dornheim[†], Jan Vorberger*, Kushal Ramakrishna*,
Zhandos Moldabekov**, Alexey Filinov, and Shen Zhang,

in collaboration with Travis Sjostrom¹, Fionn D. Malone², W.M.C. Foulkes³, and Frank Graziani²

Institute of Theoretical Physics and Astrophysics, Kiel University

[†] Center for Advanced Systems Understanding, * Helmholtz-Zentrum Dresden

** Al Farabi University, Almaty, Kazakhstan

¹Theoretical Division Los Alamos National Laboratory, Los Alamos, New Mexico, USA

²Lawrence Livermore National Lab

³Department of Physics, Imperial College London, UK

October 2019

DFG

DAAD



Introduction: warm dense matter

Warm dense matter (WDM):

- ▶ Nearly classical ions
- ▶ Degenerate non-ideal electrons
- ▶ Coupling parameter:

$$r_s = \frac{\bar{r}}{a_B} \sim 0.1 \dots 10$$

- ▶ Degeneracy parameter:

$$\theta = T/T_F \sim 0.1 \dots 10$$

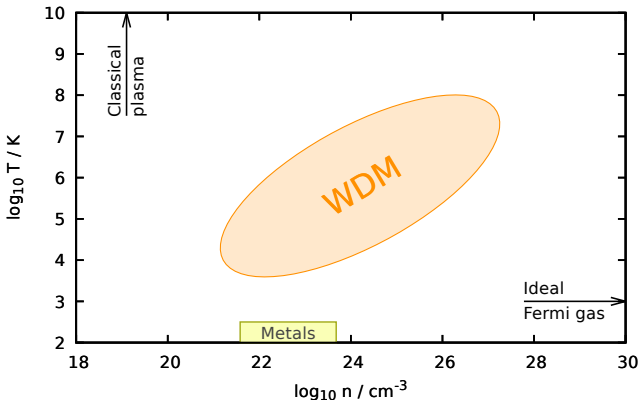


Figure: From T. Dornheim, S. Groth, and M. Bonitz, *Physics Reports* **744**, 1-86 (2018)

Introduction: warm dense matter

Warm dense matter (WDM):

- ▶ Nearly classical ions
- ▶ Degenerate non-ideal electrons
- ▶ Coupling parameter:

$$r_s = \frac{\bar{r}}{a_B} \sim 0.1 \dots 10$$

- ▶ Degeneracy parameter:

$$\theta = T/T_F \sim 0.1 \dots 10$$

- ▶ Temperature, degeneracy and coupling effects equally important
→ No small parameters

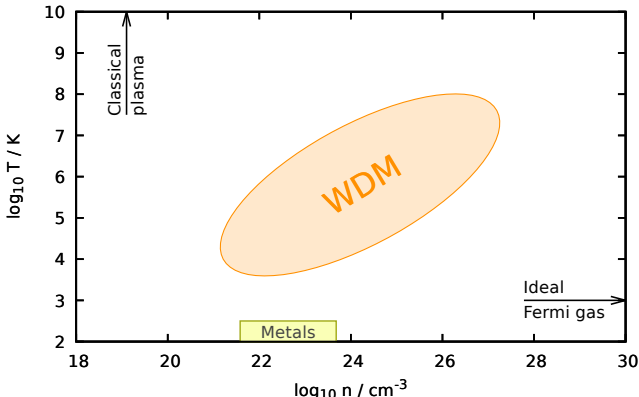


Figure: From T. Dornheim, S. Groth, and M. Bonitz, *Physics Reports* **744**, 1-86 (2018)

Introduction: warm dense matter

Warm dense matter (WDM):

- ▶ Nearly classical ions
- ▶ Degenerate non-ideal electrons
- ▶ Coupling parameter:

$$r_s = \frac{\bar{r}}{a_B} \sim 0.1 \dots 10$$

- ▶ Degeneracy parameter:

$$\theta = T/T_F \sim 0.1 \dots 10$$

- ▶ Temperature, degeneracy and coupling effects equally important
→ No small parameters

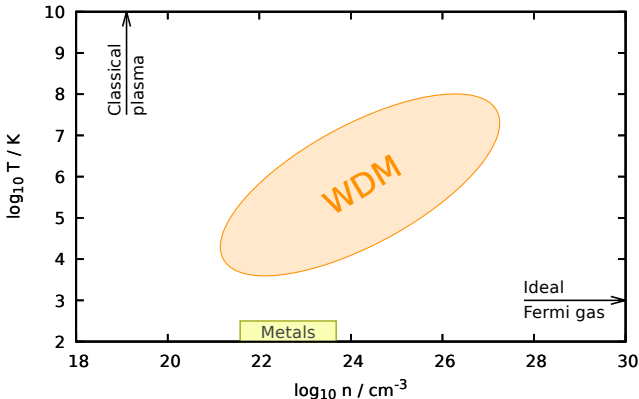


Figure: From T. Dornheim, S. Groth, and M. Bonitz, *Physics Reports* **744**, 1-86 (2018)

Perturbation theory and ground-state approaches fail

Theoretical problems and simulation methods for WDM

1. WDM in equilibrium

- ▶ multiple components free electrons, ions, atoms, and (highly excited) solid
- ▶ ⇒ accessible only by DFT+MD

Problems of DFT:

- ▶ assumes electrons in ground state
- ▶ poor electronic correlations, binding energies, band gaps etc.
- ▶ ⇒ accurate static input: QMC

2. WDM out of equilibrium

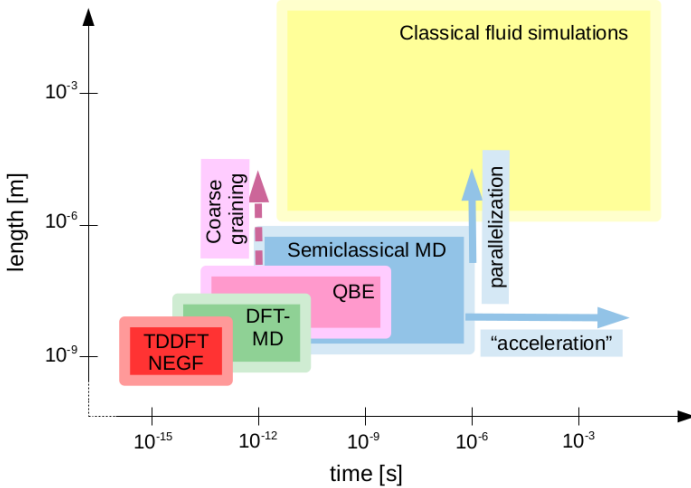


Figure: modified from M. Bonitz *et al.*, *Front. Chem. Science Engin.* (2019)
QBE: quantum Boltzmann equation, NEGFL: Nonequilibrium Green functions

Theoretical problems and simulation methods for WDM

1. WDM in equilibrium

- ▶ multiple components free electrons, ions, atoms, and (highly excited) solid
- ▶ ⇒ accessible only by DFT+MD

Problems of DFT:

- ▶ assumes electrons in ground state
- ▶ poor electronic correlations, binding energies, band gaps etc.
- ▶ ⇒ accurate static input: QMC

2. WDM out of equilibrium

- ▶ fluid simulations (long scales)
- ▶ time-dependent DFT (same problems as DFT), quantum kinetic theory, Nonequilibrium Green functions

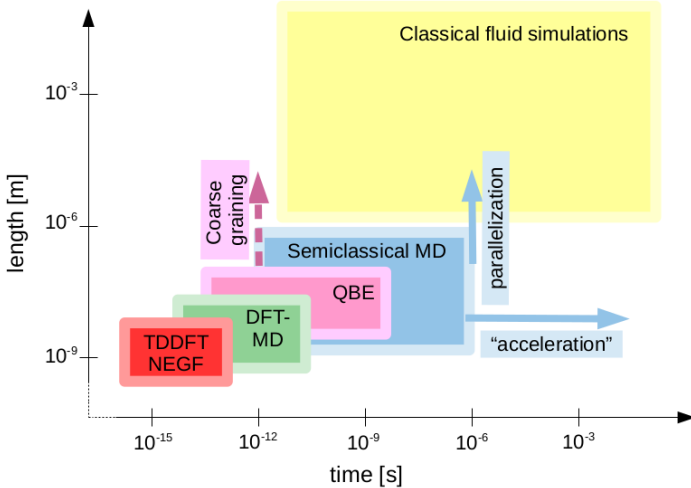


Figure: modified from M. Bonitz *et al.*, *Front. Chem. Science Engin.* (2019)
QBE: quantum Boltzmann equation, NEG: Nonequilibrium Green functions

Theoretical problems and simulation methods for WDM

1. WDM in equilibrium

- ▶ multiple components free electrons, ions, atoms, and (highly excited) solid
- ▶ ⇒ accessible only by DFT+MD

Problems of DFT:

- ▶ assumes electrons in ground state
- ▶ poor electronic correlations, binding energies, band gaps etc.
- ▶ ⇒ accurate static input: QMC

2. WDM out of equilibrium

- ▶ fluid simulations (long scales)
- ▶ time-dependent DFT (same problems as DFT), quantum kinetic theory, Nonequilibrium Green functions
- ▶ complementary strengths and limitations need combination of methods

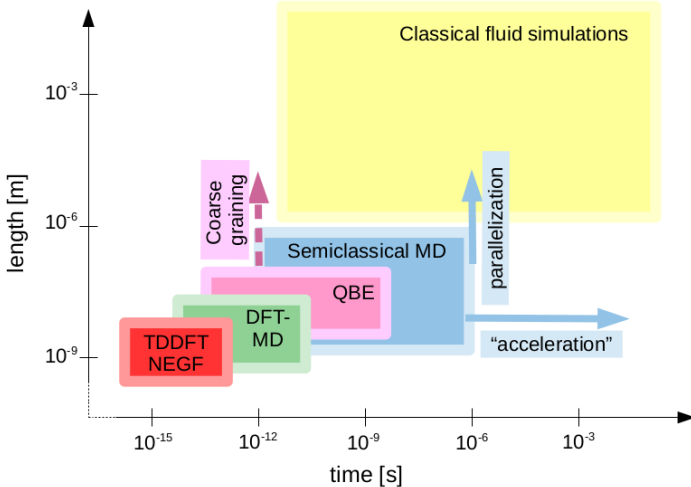


Figure: modified from M. Bonitz et al., *Front. Chem. Science Engin.* (2019)
QBE: quantum Boltzmann equation, NEG F: Nonequilibrium Green functions

Importance of the uniform electron gas (UEG)

Model system of Coulomb interacting quantum electrons in a uniform positive background

Ground state ($T = 0$):

- ▶ Simple model for conduction electrons in metals
- ▶ **Exchange-correlation (XC) energy:**

$$e_{\text{xc}}(r_s) = e_{\text{tot}}(r_s) - e_0(r_s)$$

→ Input for density functional theory (DFT) simulations (in LDA and GGA)

→ Parametrization¹ of $e_{\text{xc}}(r_s)$ from ground state quantum Monte Carlo data²

¹ J.P. Perdew and A. Zunger, PRB **23**, 5048 (1981)

² D.M. Ceperley and B. Alder, PRL **45**, 566 (1980)

³ N.D. Mermin, Phys. Rev **137**, A1441 (1965)

⁴ A.Y. Potekhin and G. Chabrier, A&A **550**, A43 (2013)

Importance of the uniform electron gas (UEG)

Model system of Coulomb interacting quantum electrons in a uniform positive background

Ground state ($T = 0$):

- ▶ Simple model for conduction electrons in metals
- ▶ **Exchange-correlation (XC) energy:**

$$e_{\text{xc}}(r_s) = e_{\text{tot}}(r_s) - e_0(r_s)$$

- Input for density functional theory (DFT) simulations (in LDA and GGA)
- Parametrization¹ of $e_{\text{xc}}(r_s)$ from ground state quantum Monte Carlo data²

Warm dense matter ($T \sim T_F$):

- ▶ **Thermal DFT**³: minimize free energy $F = E - TS$
 - Requires parametrization of XC free energy of UEG:

$$f_{\text{xc}}(r_s, \theta) = f_{\text{tot}}(r_s, \theta) - f_0(r_s, \theta)$$

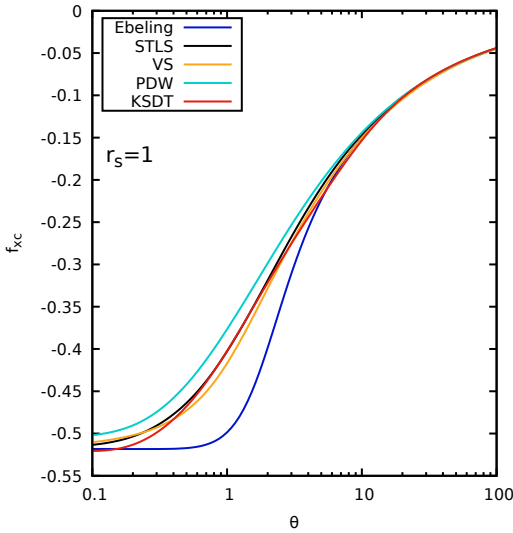
- ▶ $f_{\text{xc}}(r_s, \theta)$ direct input for **EOS models** of astrophysical objects⁴
- ▶ $f_{\text{xc}}(r_s, \theta)$ contains **complete thermodynamic information** of UEG

¹ J.P. Perdew and A. Zunger, PRB **23**, 5048 (1981) ² D.M. Ceperley and B. Alder, PRL **45**, 566 (1980) ³ N.D. Mermin, Phys. Rev **137**, A1441 (1965)

⁴ A.Y. Potekhin and G. Chabrier, A&A **550**, A43 (2013)

Many parametrizations for f_{xc} based on different approximate approaches:

- ▶ Semi-analytical approaches by **Ebeling**¹
- ▶ Dielectric methods, e.g. Singwi-Tosi-Land-Sjölander² (**STLS**) and Vashista-Singwi³ (**VS**)
- ▶ Quantum-classical mappings, e.g. Perrot and Dharma-wardana⁴ (**PDW**)
- ▶ **Most recent:** Fit by Karasiev⁵ *et al.* (**KSDT**) to Restricted Path Integral Monte Carlo (**RPIMC**) data⁶



¹ W. Ebeling and H. Lehmann, Ann. Phys. **45**, (1988)

² S. Ichimaru, H. Iyetomi, and S. Tanaka, Phys. Rep. **149**, (1987)

³ T. Sjostrom and J. Dufty, PRB **88**, (2013)

⁴ F. Perrot and MWC Dharma-wardana, PRB **62**, (2000)

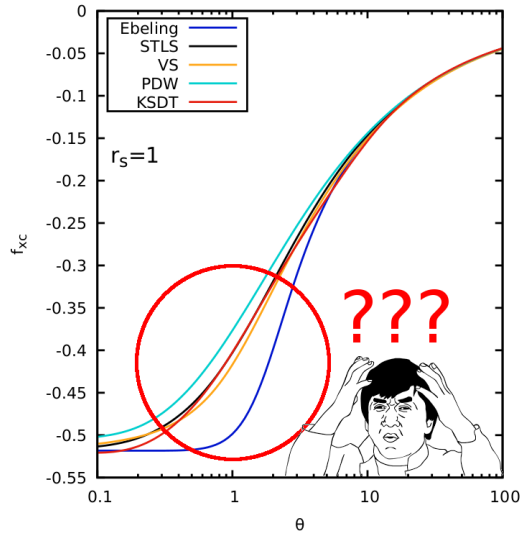
⁵ V.V. Karasiev *et al.*, PRL **112**, (2014)

⁶ E.W. Brown *et al.*, PRL **110**, (2013)

Many parametrizations for f_{xc} based on different approximate approaches:

- ▶ Semi-analytical approaches by **Ebeling**¹
- ▶ Dielectric methods, e.g. Singwi-Tosi-Land-Sjölander² (**STLS**) and Vashista-Singwi³ (**VS**)
- ▶ Quantum-classical mappings, e.g. Perrot and Dharma-wardana⁴ (**PDW**)
- ▶ **Most recent:** Fit by Karasiev⁵ *et al.* (**KSDT**) to Restricted Path Integral Monte Carlo (**RPIMC**) data⁶

**Accuracy of existing parametrizations
for $f_{xc}(r_s, \theta)$ unclear**



¹ W. Ebeling and H. Lehmann, Ann. Phys. **45**, (1988)

² S. Ichimaru, H. Iyetomi, and S. Tanaka, Phys. Rep. **149**, (1987)

³ T. Sjostrom and J. Dufty, PRB **88**, (2013)

⁴ F. Perrot and MWC Dharma-wardana, PRB **62**, (2000)

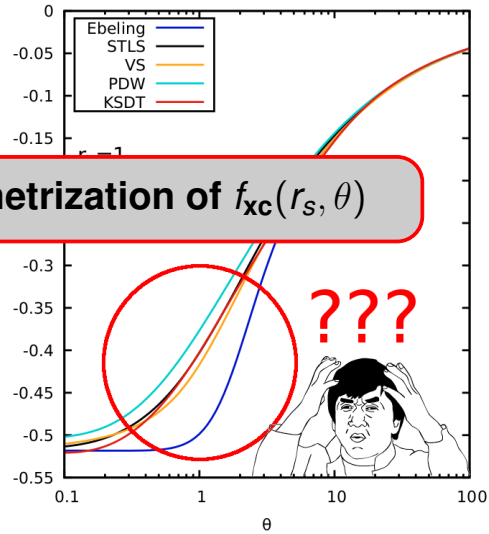
⁵ V.V. Karasiev *et al.*, PRL **112**, (2014)

⁶ E.W. Brown *et al.*, PRL **110**, (2013)

Many parametrizations for f_{xc} based on different approximate approaches:

- ▶ Semi-analytical approaches by **Ebeling**¹
- ▶ Dielectric methods, e.g. Singwi-Tosi-Land-Sjölander² (**STLS**) a
- ▶ Quantum Dharma-
- ▶ **Most recent:** Fit by Karasiev⁵ *et al.* (**KSDT**) to Restricted Path Integral Monte Carlo (**RPIMC**) data⁶

**Accuracy of existing parametrizations
for $f_{xc}(r_s, \theta)$ unclear**



¹ W. Ebeling and H. Lehmann, Ann. Phys. **45**, (1988)

² S. Ichimaru, H. Iyetomi, and S. Tanaka, Phys. Rep. **149**, (1987)

³ T. Sjostrom and J. Dufty, PRB **88**, (2013)

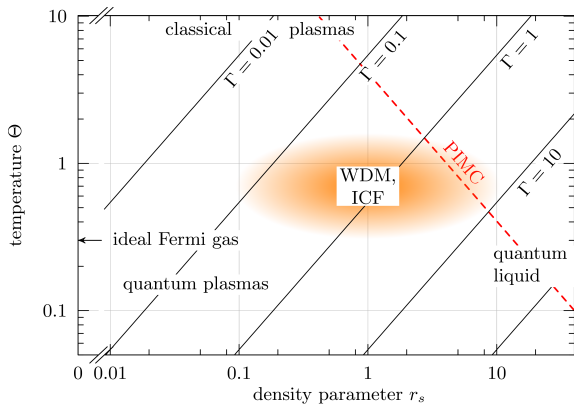
⁴ F. Perrot and MWC Dharma-wardana, PRB **62**, (2000)

⁵ V.V. Karasiev *et al.*, PRL **112**, (2014)

⁶ E.W. Brown *et al.*, PRL **110**, (2013)

Path integral Monte Carlo (PIMC) simulation of the warm dense UEG

- Standard PIMC in warm dense regime severely hampered by ***fermion sign problem***:



¹ E.W. Brown *et al.*, PRL **110**, 146405 (2013)

² T. Schoof *et al.*, Phys. Rev. Lett **115**, 130402 (2015)

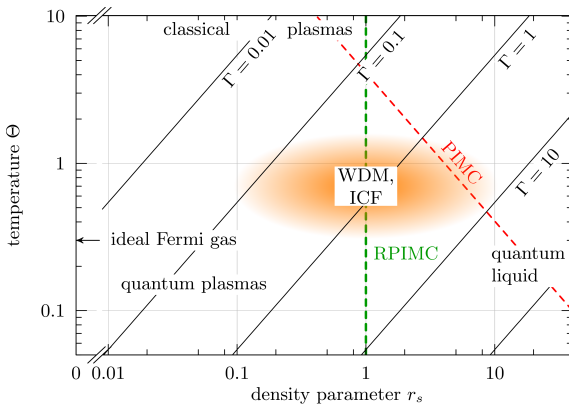
³ T. Schoof *et al.*, Contrib. Plasma Phys. **51**, 687 (2011)

⁴ T. Dornheim *et al.*, New J. Phys. **17**, 073017 (2015)

⁵ T. Dornheim *et al.*, J. Chem. Phys. **143**, 204101 (2015)

Path integral Monte Carlo (PIMC) simulation of the warm dense UEG

- ▶ Standard PIMC in warm dense regime severely hampered by ***fermion sign problem***:
 - ▶ First results¹ by E. Brown, D. Ceperley *et al.* (2013) based on ***fixed node approximation (RPIMC)***
 - ▶ Induces **systematic errors** of unknown magnitude
 - ▶ **RPIMC** limited to $r_s \gtrsim 1$



¹ E.W. Brown *et al.*, PRL **110**, 146405 (2013)

² T. Schoof *et al.*, Phys. Rev. Lett **115**, 130402 (2015)

³ T. Schoof *et al.*, Contrib. Plasma Phys. **51**, 687 (2011)

⁴ T. Dornheim *et al.*, New J. Phys. **17**, 073017 (2015)

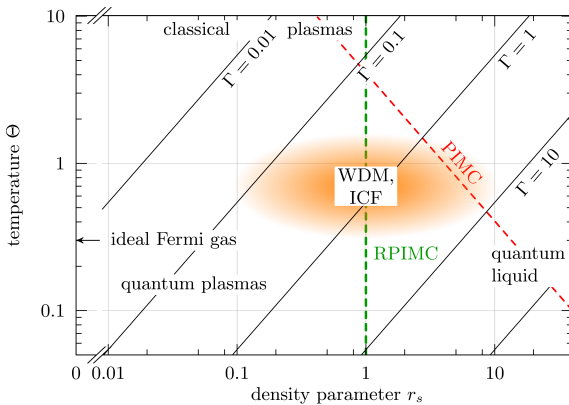
⁵ T. Dornheim *et al.*, J. Chem. Phys. **143**, 204101 (2015)

Path integral Monte Carlo (PIMC) simulation of the warm dense UEG

- ▶ Standard PIMC in warm dense regime severely hampered by ***fermion sign problem***:
 - ▶ First results¹ by E. Brown, D. Ceperley *et al.* (2013) based on ***fixed node approximation (RPIMC)***
 - ▶ Induces **systematic errors** of unknown magnitude
 - ▶ RPIMC limited to $r_s \gtrsim 1$

Our approach:

Avoid fermion sign problem by combining two exact and complementary QMC methods:



¹ E.W. Brown *et al.*, PRL **110**, 146405 (2013)

² T. Schoof *et al.*, Phys. Rev. Lett **115**, 130402 (2015)

³ T. Schoof *et al.*, Contrib. Plasma Phys. **51**, 687 (2011)

⁴ T. Dornheim *et al.*, New J. Phys. **17**, 073017 (2015)

⁵ T. Dornheim *et al.*, J. Chem. Phys. **143**, 204101 (2015)

Path integral Monte Carlo (PIMC) simulation of the warm dense UEG

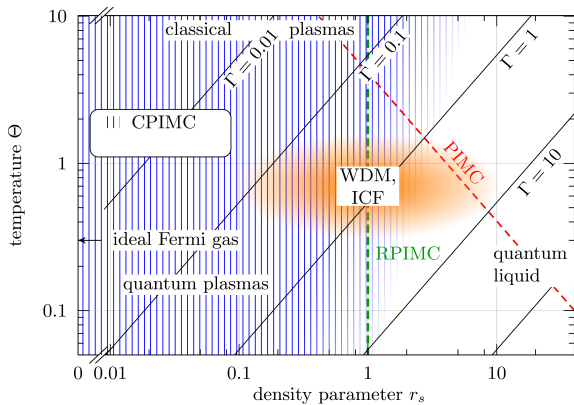
- ▶ Standard PIMC in warm dense regime severely hampered by **fermion sign problem**:
 - ▶ First results¹ by E. Brown, D. Ceperley *et al.* (2013) based on **fixed node approximation (RPIMC)**
 - ▶ Induces **systematic errors** of unknown magnitude
 - ▶ RPIMC limited to $r_s \gtrsim 1$

Our approach:

Avoid fermion sign problem by combining two exact and complementary QMC methods:

1. Configuration PIMC (CPIMC)^{2,3}

→ Excels at high density $r_s \lesssim 1$ and strong degeneracy



¹ E.W. Brown *et al.*, PRL **110**, 146405 (2013)

² T. Schoof *et al.*, Phys. Rev. Lett **115**, 130402 (2015)

³ T. Schoof *et al.*, Contrib. Plasma Phys. **51**, 687 (2011)

⁴ T. Dornheim *et al.*, New J. Phys. **17**, 073017 (2015)

⁵ T. Dornheim *et al.*, J. Chem. Phys. **143**, 204101 (2015)

Path integral Monte Carlo (PIMC) simulation of the warm dense UEG

- ▶ Standard PIMC in warm dense regime severely hampered by ***fermion sign problem***:
 - ▶ First results¹ by E. Brown, D. Ceperley *et al.* (2013) based on ***fixed node approximation (RPIMC)***
 - ▶ Induces **systematic errors** of unknown magnitude
 - ▶ RPIMC limited to $r_s \gtrsim 1$

Our approach:

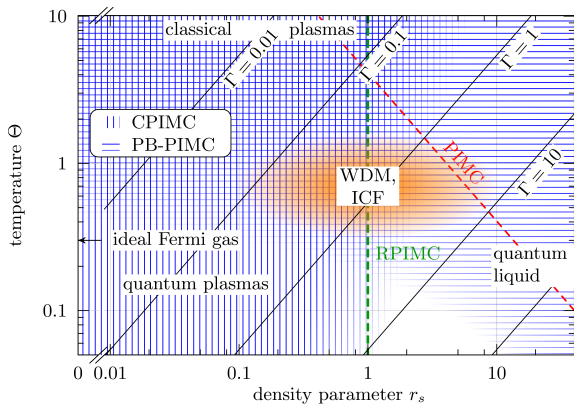
Avoid fermion sign problem by combining two exact and complementary QMC methods:

1. Configuration PIMC (CPIMC)^{2,3}

→ Excels at high density $r_s \lesssim 1$ and strong degeneracy

2. Permutation blocking PIMC (PB-PIMC)^{4,5}

→ Extends standard PIMC towards stronger degeneracy



¹ E.W. Brown *et al.*, PRL **110**, 146405 (2013)

² T. Schoof *et al.*, Phys. Rev. Lett **115**, 130402 (2015)

³ T. Schoof *et al.*, Contrib. Plasma Phys. **51**, 687 (2011)

⁴ T. Dornheim *et al.*, New J. Phys. **17**, 073017 (2015)

⁵ T. Dornheim *et al.*, J. Chem. Phys. **143**, 204101 (2015)

Path integral Monte Carlo (PIMC) simulation of the warm dense UEG

- Standard PIMC in warm dense regime severely hampered by ***fermion sign problem***:
 - First results¹ by E. Brown, D. Ceperley *et al.* (2013) based on ***fixed node approximation (RPIMC)***
 - Induces ***systematic errors*** of unknown magnitude
 - ***RPIMC*** limited to $r_s \gtrsim 1$

Our approach:

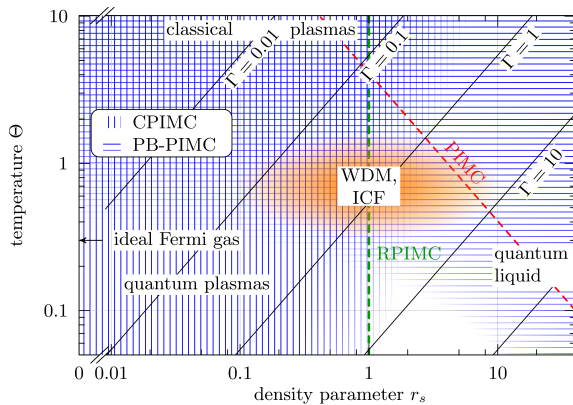
Avoid fermion sign problem by combining two exact and complementary QMC methods:

1. Configuration PIMC (CPIMC)^{2,3}

→ Excels at high density $r_s \lesssim 1$ and strong degeneracy

2. Permutation blocking PIMC (PB-PIMC)^{4,5}

→ Extends standard PIMC towards stronger degeneracy



Ab initio simulations over broad range of parameters

¹ E.W. Brown *et al.*, PRL **110**, 146405 (2013)

² T. Schoof *et al.*, Phys. Rev. Lett **115**, 130402 (2015)

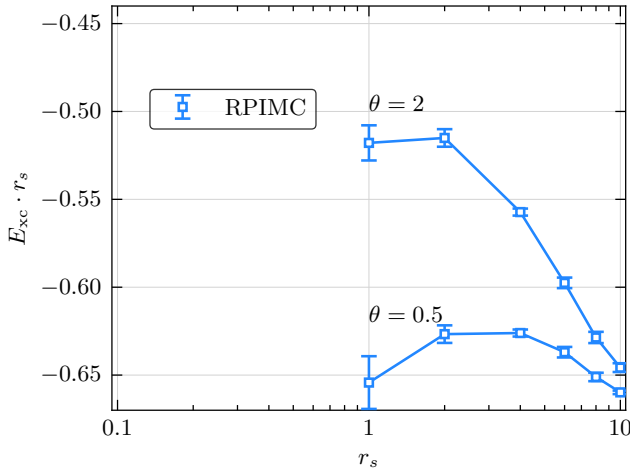
³ T. Schoof *et al.*, Contrib. Plasma Phys. **51**, 687 (2011)

⁴ T. Dornheim *et al.*, New J. Phys. **17**, 073017 (2015)

⁵ T. Dornheim *et al.*, J. Chem. Phys. **143**, 204101 (2015)

Exact exchange-correlation energy $E_{xc} = E - E_0$ (E_0 : ideal energy)
 $(N = 33$ spin-polarized electrons, $\theta \geq 0.5$, $\forall r_s$)

- RPIMC limited to $r_s \geq 1$



¹S. Groth *et al.*, Phys. Rev. B **93**, 085102 (2016)

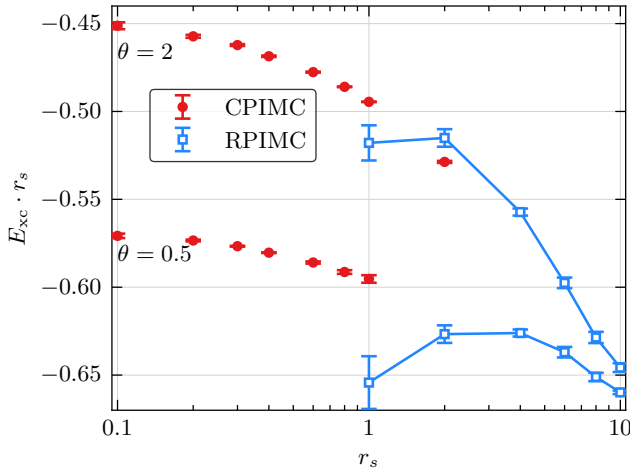
²T. Dornheim *et al.*, Phys. Rev. B **93**, 205134 (2016)

³F.D. Malone *et al.*, Phys. Rev. Lett. **117**, 115701 (2016)

⁴T. Schoof *et al.*, Phys. Rev. Lett. (2015)

Exact exchange-correlation energy $E_{xc} = E - E_0$ (E_0 : ideal energy)
 $(N = 33$ spin-polarized electrons, $\theta \geq 0.5$, $\forall r_s$)

- **RPIMC** limited to $r_s \geq 1$
- **CPIMC** excels at high density



¹S. Groth *et al.*, Phys. Rev. B **93**, 085102 (2016)

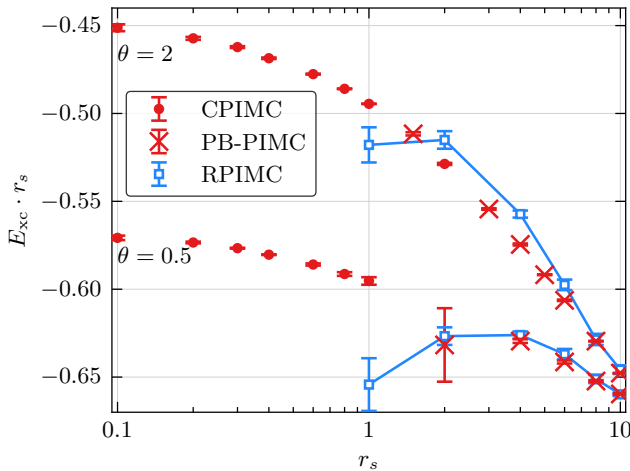
²T. Dornheim *et al.*, Phys. Rev. B **93**, 205134 (2016)

³F.D. Malone *et al.*, Phys. Rev. Lett. **117**, 115701 (2016)

⁴T. Schoof *et al.*, Phys. Rev. Lett. (2015)

Exact exchange-correlation energy $E_{xc} = E - E_0$ (E_0 : ideal energy)
 $(N = 33$ spin-polarized electrons, $\theta \geq 0.5$, $\forall r_s$)

- **RPIMC** limited to $r_s \geq 1$
- **CPIMC** excels at high density
- **PB-PIMC** applicable at $\theta \gtrsim 0.5$



¹S. Groth *et al.*, Phys. Rev. B **93**, 085102 (2016)

²T. Dornheim *et al.*, Phys. Rev. B **93**, 205134 (2016)

³F.D. Malone *et al.*, Phys. Rev. Lett. **117**, 115701 (2016)

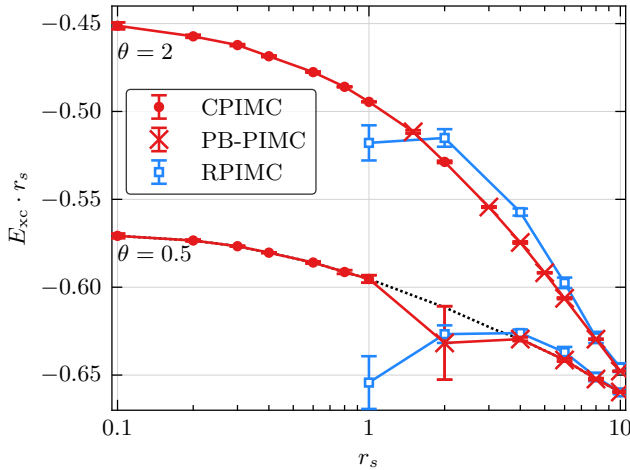
⁴T. Schoof *et al.*, Phys. Rev. Lett. (2015)

Exact exchange-correlation energy $E_{xc} = E - E_0$ (E_0 : ideal energy)
 $(N = 33$ spin-polarized electrons, $\theta \geq 0.5$, $\forall r_s$)

- **RPIMC** limited to $r_s \geq 1$
- **CPIMC** excels at high density
- **PB-PIMC** applicable at $\theta \gtrsim 0.5$

Combination¹ yields exact results over entire density range down to $\theta \sim 0.5$

- Also applies to the **unpolarized UEG**²
- confirmed by independent **DMQMC** simulations³



¹S. Groth *et al.*, Phys. Rev. B **93**, 085102 (2016)

²T. Dornheim *et al.*, Phys. Rev. B **93**, 205134 (2016)

³F.D. Malone *et al.*, Phys. Rev. Lett. **117**, 115701 (2016)

⁴T. Schoof *et al.*, Phys. Rev. Lett. (2015)

The first complete *ab initio*-based thermodynamic data for the UEG
at WDM conditions: $0 \leq r_s \leq 20$, $0 \leq \Theta \leq 10$, $0 \leq \xi \leq 1$, error below 0.3%

1. Accurate results for f_{xc} for finite N for paramagnetic and ferromagnetic cases^{1,2}

¹T. Schoof *et al.*, PRL **115**, 130402 (2015) ²S. Groth *et al.*, PRB **93**, 085102 (2016) ⁵T. Dornheim *et al.*, Phys. Plasmas **24**, 056303 (2017)

³ T. Dornheim *et al.*, PRL **117**, 156403 (2016) ⁴ S. Groth *et al.*, PRL **119**, 135001 (2017) ⁶T. Dornheim, S. Groth, and M. Bonitz, *Physics Reports* **744**, 1-86 (2018)

⁷ V. Karasiev *et al.*, Phys. Rev. B (2019): in part incorrect statements; ⁸ T. Dornheim *et al.*, Phys. Rev. Lett. (2018)

The first complete *ab initio*-based thermodynamic data for the UEG
at WDM conditions: $0 \leq r_s \leq 20$, $0 \leq \Theta \leq 10$, $0 \leq \xi \leq 1$, error below 0.3%

1. Accurate results for f_{xc} for finite N for paramagnetic and ferromagnetic cases^{1,2}
2. Accurate finite size corrections and extrapolation to thermodynamic limit³, $N \rightarrow \infty$
3. Connect our data to ground state data, cover entire temperature range⁴

¹T. Schoof *et al.*, PRL **115**, 130402 (2015) ²S. Groth *et al.*, PRB **93**, 085102 (2016) ⁵T. Dornheim *et al.*, Phys. Plasmas **24**, 056303 (2017)

³ T. Dornheim *et al.*, PRL **117**, 156403 (2016) ⁴ S. Groth *et al.*, PRL **119**, 135001 (2017) ⁶T. Dornheim, S. Groth, and M. Bonitz, *Physics Reports* **744**, 1-86 (2018)

⁷ V. Karasiev *et al.*, Phys. Rev. B (2019): in part incorrect statements; ⁸ T. Dornheim *et al.*, Phys. Rev. Lett. (2018)

The first complete *ab initio*-based thermodynamic data for the UEG
at WDM conditions: $0 \leq r_s \leq 20$, $0 \leq \Theta \leq 10$, $0 \leq \xi \leq 1$, error below 0.3%

1. Accurate results for f_{xc} for finite N for paramagnetic and ferromagnetic cases^{1,2}
2. Accurate finite size corrections and extrapolation to thermodynamic limit³, $N \rightarrow \infty$
3. Connect our data to ground state data, cover entire temperature range⁴
4. New data for intermediate spin polarizations^{4,6}, 3-dimensional analytical parametrization⁷, $f_{xc}(r_s, \Theta, \xi)$
 f_{xc} -functional implemented in [Libxc](#) (LDA_XC_GDSMFB)

Comments and outlook:

- ▶ first unbiased tests of many earlier models and fits^{5,6}: STLS, VS, Ichimaru, Dharma wardana, Ebeling, Green functions (Kraeft, Vorberger, Rehr...) etc.: benchmark data allow for model improvement
- ▶ earlier fit (KSDT) by Karasiev *et al.*: tested and subsequently corrected, *now good agreement* with GDSMFB

¹T. Schoo *et al.*, PRL **115**, 130402 (2015) ²S. Groth *et al.*, PRB **93**, 085102 (2016) ⁵T. Dornheim *et al.*, Phys. Plasmas **24**, 056303 (2017)

³T. Dornheim *et al.*, PRL **117**, 156403 (2016) ⁴S. Groth *et al.*, PRL **119**, 135001 (2017) ⁶T. Dornheim, S. Groth, and M. Bonitz, *Physics Reports* **744**, 1-86 (2018)

⁷V. Karasiev *et al.*, Phys. Rev. B (2019): in part incorrect statements; ⁸T. Dornheim *et al.*, Phys. Rev. Lett. (2018)

The first complete *ab initio*-based thermodynamic data for the UEG
at WDM conditions: $0 \leq r_s \leq 20$, $0 \leq \Theta \leq 10$, $0 \leq \xi \leq 1$, error below 0.3%

1. Accurate results for f_{xc} for finite N for paramagnetic and ferromagnetic cases^{1,2}
2. Accurate finite size corrections and extrapolation to thermodynamic limit³, $N \rightarrow \infty$
3. Connect our data to ground state data, cover entire temperature range⁴
4. New data for intermediate spin polarizations^{4,6}, 3-dimensional analytical parametrization⁷, $f_{xc}(r_s, \Theta, \xi)$
 f_{xc} -functional implemented in [Libxc](#) (LDA_XC_GDSMFB)

Comments and outlook:

- ▶ first unbiased tests of many earlier models and fits^{5,6}: STLS, VS, Ichimaru, Dharma wardana, Ebeling, Green functions (Kraeft, Vorberger, Rehr...) etc.: benchmark data allow for model improvement
- ▶ earlier fit (KSDT) by Karasiev *et al.*: tested and subsequently corrected, *now good agreement* with GDSMFB
- ▶ derivatives $\partial f_{xc}/\partial n$ and $\partial f_{xc}/\partial T$ potentially inaccurate; \Rightarrow *fits to separate ab initio data needed*

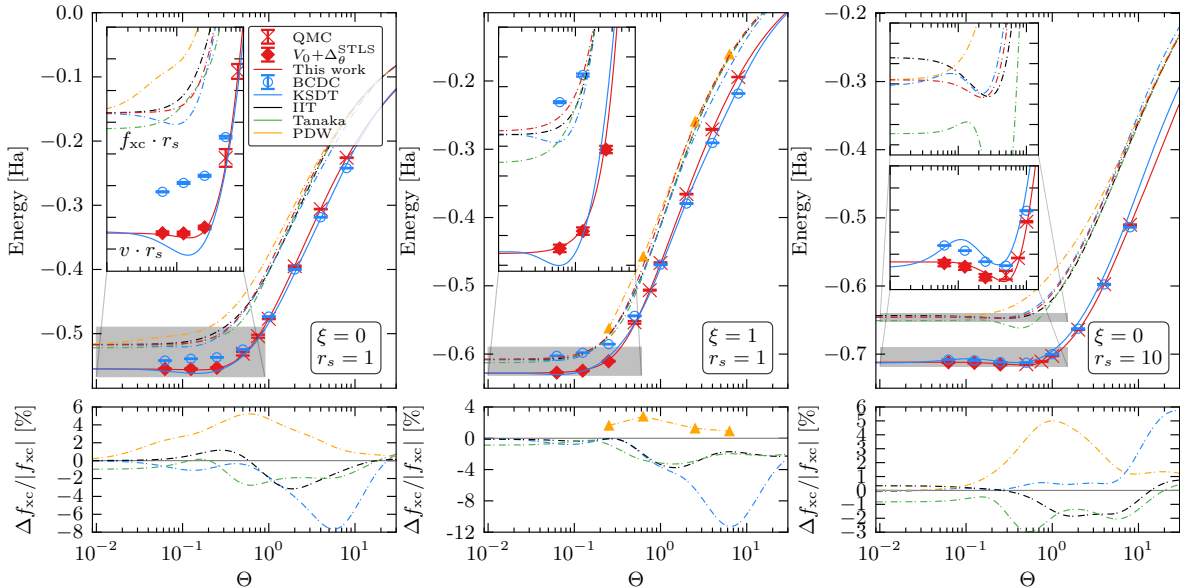
¹T. Schoo *et al.*, PRL **115**, 130402 (2015) ²S. Groth *et al.*, PRB **93**, 085102 (2016) ⁵T. Dornheim *et al.*, Phys. Plasmas **24**, 056303 (2017)

³T. Dornheim *et al.*, PRL **117**, 156403 (2016) ⁴S. Groth *et al.*, PRL **119**, 135001 (2017) ⁶T. Dornheim, S. Groth, and M. Bonitz, *Physics Reports* **744**, 1-86 (2018)

⁷V. Karasiev *et al.*, Phys. Rev. B (2019): in part incorrect statements; ⁸T. Dornheim *et al.*, Phys. Rev. Lett. (2018)

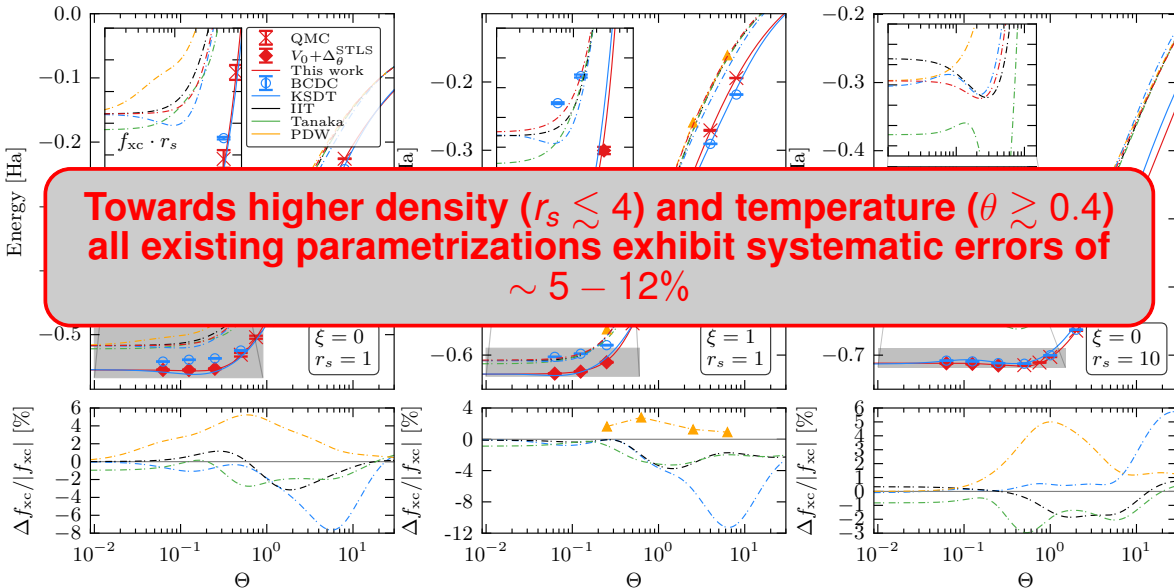
Benchmarks for existing and future models and fits:

S. Groth *et al.*, PRL (2017)

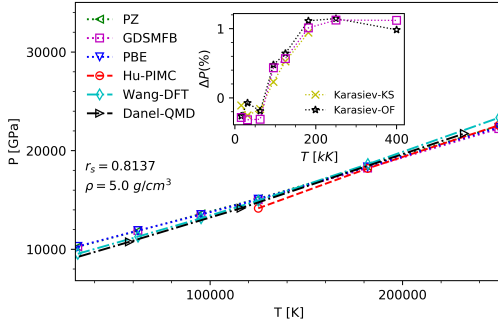
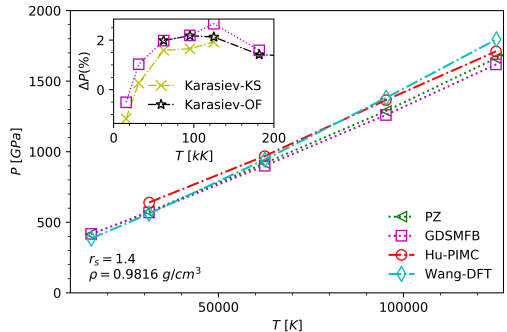


Benchmarks for existing and future models and fits:

S. Groth *et al.*, PRL (2017)



Impact of finite-T functional on DFT-MD simulations: dense hydrogen¹



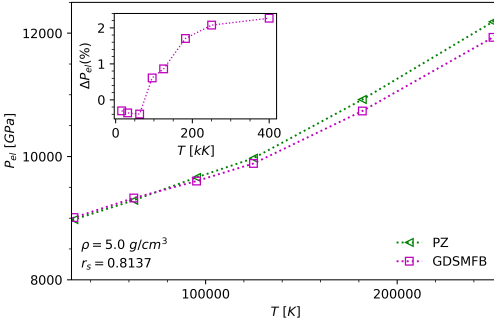
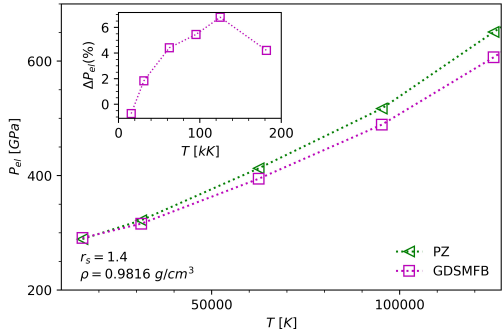
GDSMFB: present finite-T functional, **PZ:** Perdew, Zunger (1981), **PBE:** Perdew, Burke, Enzerhof (1996)

Hu-PIMC: Hu, Militzer, PRB 2011; **Wang-DFT:** Orbital-free MD, Phys. Plasmas (2013)

Karasiev et al., PRE (2016)

¹Kushal Ramakrishna, unpublished

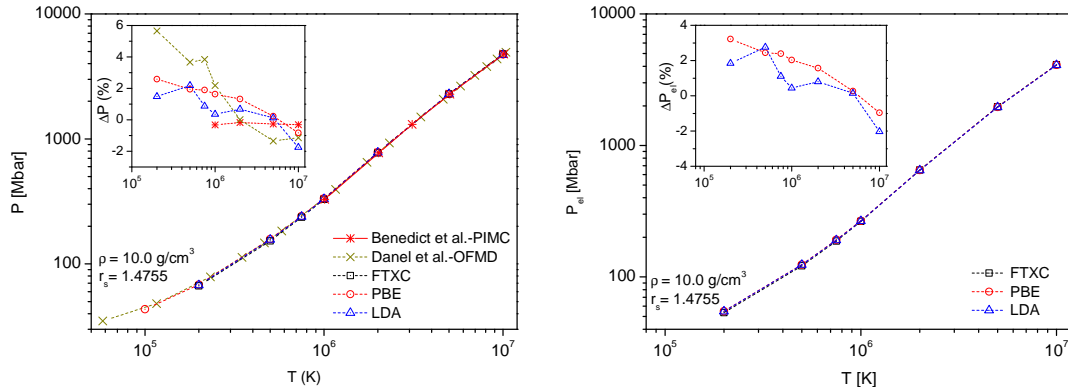
Impact of finite-T functional: dense hydrogen, electronic pressure²



significantly larger differences in specific heat, susceptibilities

Impact of finite-T functional on DFT-MD simulations: dense carbon³, $r_s \approx 1.5$

total pressure (left) vs. electronic pressure, $E_F \approx 23\text{eV} \approx 267,000\text{K}$



baseline=FTXC: present finite-T functional (GDSMFB), compared to $T = 0$ **PBE** and **LDA**

Danel: Danel, Kazandjian, Piron, PRE 2018;

Benedict: Benedict, Driver, Hamel, Militzer, Qi, Correa, Saul, and Schwegler, Phys. Rev. B (2014)

³Shen Zhang, unpublished (highly efficient high- T approach)

Ab initio dynamic (ω -dependent) results for the warm dense UEG

- ▶ **Key quantity:** dynamic structure factor

$$S(\mathbf{q}, \omega) := \frac{1}{2\pi} \int_{-\infty}^{\infty} dt \underbrace{\langle \hat{n}_{\mathbf{q}}(t) \hat{n}_{-\mathbf{q}}(0) \rangle}_{:= F(\mathbf{q}, t)} e^{i\omega t}$$

→ Directly measured in **scattering experiments**

Ab initio dynamic (ω -dependent) results for the warm dense UEG

- ▶ **Key quantity:** dynamic structure factor

$$S(\mathbf{q}, \omega) := \frac{1}{2\pi} \int_{-\infty}^{\infty} dt \underbrace{\langle \hat{n}_{\mathbf{q}}(t) \hat{n}_{-\mathbf{q}}(0) \rangle}_{:= F(\mathbf{q}, t)} e^{i\omega t}$$

→ Directly measured in **scattering experiments**

- ▶ **Chihara decomposition** applies for non-collective scattering:

$$S(\mathbf{q}, \omega) = S_{\text{b-b}}(\mathbf{q}, \omega) + S_{\text{b-f}}(\mathbf{q}, \omega) + S_{\text{f-f}}(\mathbf{q}, \omega)$$

$$\rightarrow S_{\text{f-f}}(\mathbf{q}, \omega) \sim S^{\text{UEG}}(\mathbf{q}, \omega)$$

Ab initio dynamic (ω -dependent) results for the warm dense UEG

- ▶ **Key quantity:** dynamic structure factor

$$S(\mathbf{q}, \omega) := \frac{1}{2\pi} \int_{-\infty}^{\infty} dt \underbrace{\langle \hat{n}_{\mathbf{q}}(t) \hat{n}_{-\mathbf{q}}(0) \rangle}_{:=F(\mathbf{q}, t)} e^{i\omega t}$$

→ Directly measured in **scattering experiments**

- ▶ **Chihara decomposition** applies for non-collective scattering:

$$S(\mathbf{q}, \omega) = S_{\text{b-b}}(\mathbf{q}, \omega) + S_{\text{b-f}}(\mathbf{q}, \omega) + S_{\text{f-f}}(\mathbf{q}, \omega)$$

$$\rightarrow S_{\text{f-f}}(\mathbf{q}, \omega) \sim S^{\text{UEG}}(\mathbf{q}, \omega)$$

- ▶ **Practical example:** Fit model for $S(\mathbf{q}, \omega; T_e)$ to spectrum to determine electron temperature T_e

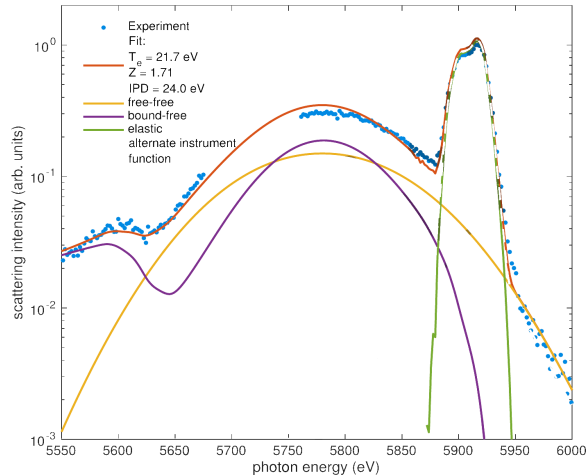


Figure: Scattering spectrum of isochorically heated graphite at LCLS. Taken from D. Kraus *et al.*, *Plasma Phys. Control. Fusion* (2019)

Ab initio dynamic (ω -dependent) results for the warm dense UEG

- ▶ **Key quantity:** dynamic structure factor

$$S(\mathbf{q}, \omega) := \frac{1}{2\pi} \int_{-\infty}^{\infty} dt \underbrace{\langle \hat{n}_{\mathbf{q}}(t) \hat{n}_{-\mathbf{q}}(0) \rangle}_{:= F(\mathbf{q}, t)} e^{i\omega t}$$

→ Directly measured in **scattering experiments**

- ▶ **Chihara decomposition** applies for non-collective scattering:

$$S(\mathbf{q}, \omega) = S_{b-b}(\mathbf{q}, \omega) + S_{b-f}(\mathbf{q}, \omega) + S_{f-f}(\mathbf{q}, \omega)$$

$$\rightarrow S_{f-f}(\mathbf{q}, \omega) \sim S^{\text{UEG}}(\mathbf{q}, \omega)$$

- ▶ **Practical example:** Fit model for $S(\mathbf{q}, \omega; T_e)$ to spectrum to determine electron temperature T_e
- ▶ **Problem:**
 $F(\mathbf{q}, t)$ requires **real time-dependent simulations**
→ with PIMC have to use analytic continuation, reconstruct $F(\mathbf{q}, it)$ and 4 frequency moments, but: insufficient information

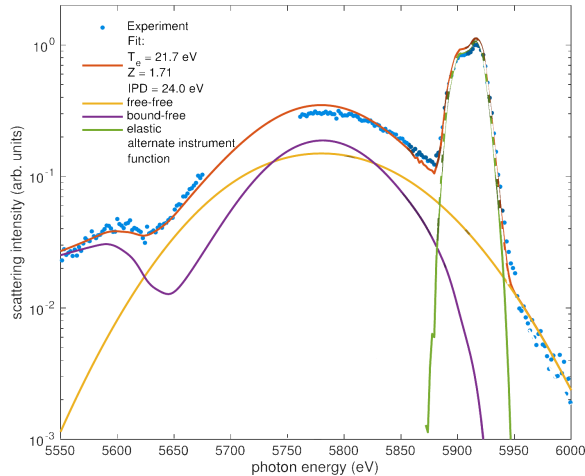


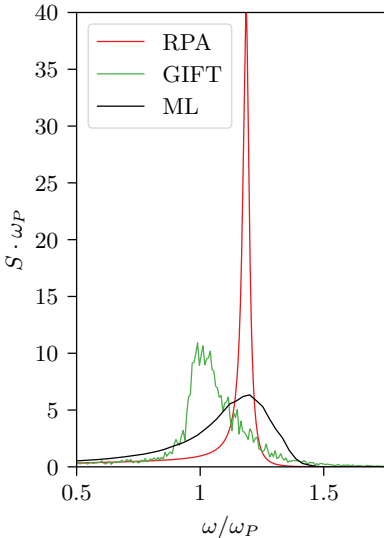
Figure: Scattering spectrum of isochorically heated graphite at LCLS. Taken from D. Kraus *et al.*, *Plasma Phys. Control. Fusion* (2019)

Incorporating additional information on $S(\mathbf{q}, \omega)$ via dielectric formulation

- ▶ Fluctuation-dissipation theorem:

$$S(\mathbf{q}, \omega) = -\frac{\text{Im}\chi(\mathbf{q}, \omega)}{\pi n(1 - e^{-\beta\omega})}$$

Dynamic structure factor of the UEG:
($\theta = 1$, $r_s = 10$, $N = 33$, $q = 0.63q_F$)



Incorporating additional information on $S(\mathbf{q}, \omega)$ via dielectric formulation

- ▶ Fluctuation-dissipation theorem:

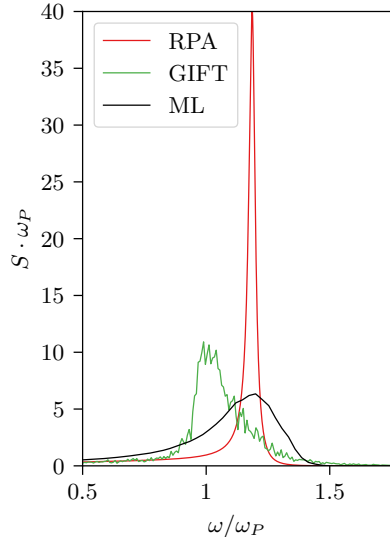
$$S(\mathbf{q}, \omega) = -\frac{\text{Im}\chi(\mathbf{q}, \omega)}{\pi n(1 - e^{-\beta\omega})}$$

- ▶ Express response function χ via ideal response function χ_0 and **dynamic local field correction** G :

$$\chi(\mathbf{q}, \omega) = \frac{\chi_0(\mathbf{q}, \omega)}{1 - v_q[1 - G(\mathbf{q}, \omega)]\chi_0(\mathbf{q}, \omega)}$$

- ▶ Random phase approximation (RPA): $G \equiv 0$

Dynamic structure factor of the UEG:
($\theta = 1$, $r_s = 10$, $N = 33$, $q = 0.63q_F$)



Incorporating additional information on $S(\mathbf{q}, \omega)$ via dielectric formulation

- ▶ Fluctuation-dissipation theorem:

$$S(\mathbf{q}, \omega) = -\frac{\text{Im}\chi(\mathbf{q}, \omega)}{\pi n(1 - e^{-\beta\omega})}$$

- ▶ Express response function χ via ideal response function χ_0 and **dynamic local field correction** G :

$$\chi(\mathbf{q}, \omega) = \frac{\chi_0(\mathbf{q}, \omega)}{1 - v_q[1 - G(\mathbf{q}, \omega)]\chi_0(\mathbf{q}, \omega)}$$

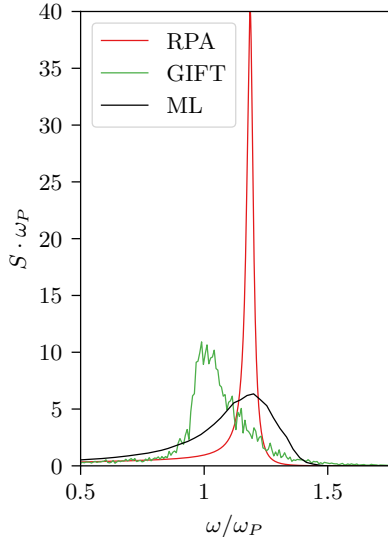
- ▶ Random phase approximation (RPA): $G \equiv 0$

Make ansatz and optimize $G(\mathbf{q}, \omega)$ instead of $S(\mathbf{q}, \omega)$

Advantages:

- ▶ Limits $G(\mathbf{q}, 0)$ and $G(\mathbf{q}, \infty)$ known from PIMC simulation
- ▶ Other exact properties of G can be incorporated

Dynamic structure factor of the UEG:
($\theta = 1$, $r_s = 10$, $N = 33$, $q = 0.63q_F$)



Incorporating additional information on $S(\mathbf{q}, \omega)$ via dielectric formulation

- ▶ Fluctuation-dissipation theorem:

$$S(\mathbf{q}, \omega) = -\frac{\text{Im}\chi(\mathbf{q}, \omega)}{\pi n(1 - e^{-\beta\omega})}$$

- ▶ Express response function χ via ideal response function χ_0 and **dynamic local field correction** G :

$$\chi(\mathbf{q}, \omega) = \frac{\chi_0(\mathbf{q}, \omega)}{1 - v_q[1 - G(\mathbf{q}, \omega)]\chi_0(\mathbf{q}, \omega)}$$

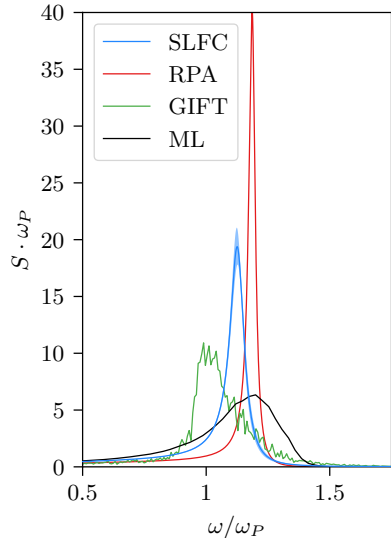
- ▶ Random phase approximation (RPA): $G \equiv 0$

Make ansatz and optimize $G(\mathbf{q}, \omega)$ instead of $S(\mathbf{q}, \omega)$

Advantages:

- ▶ Limits $G(\mathbf{q}, 0)$ and $G(\mathbf{q}, \infty)$ known from PIMC simulation
- ▶ Other exact properties of G can be incorporated

Dynamic structure factor of the UEG:
($\theta = 1$, $r_s = 10$, $N = 33$, $q = 0.63q_F$)



Incorporating additional information on $S(\mathbf{q}, \omega)$ via dielectric formulation

- ▶ Fluctuation-dissipation theorem:

$$S(\mathbf{q}, \omega) = -\frac{\text{Im} \chi(\mathbf{q}, \omega)}{i\omega}$$

- ▶ Exact dynamic spectra:
 - GIFT and ML spectra not in agreement with exact properties of $G(\mathbf{q}, \omega)$
→ to be discarded as unphysical

$$\chi(\mathbf{q}, \omega) = \frac{1}{1 - v_q [1 - G(\mathbf{q}, \omega)] \chi_0(\mathbf{q}, \omega)}$$

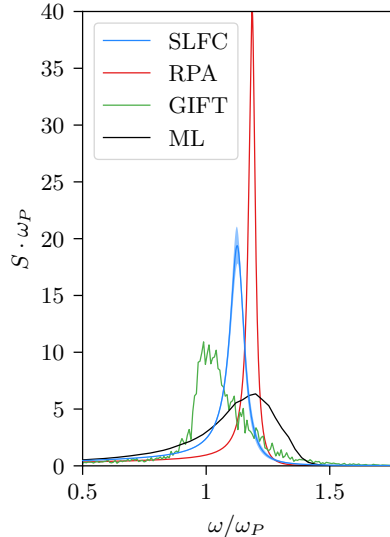
- ▶ Random phase approximation (RPA): $G \equiv 0$

Make ansatz and optimize $G(\mathbf{q}, \omega)$ instead of $S(\mathbf{q}, \omega)$

Advantages:

- ▶ Limits $G(\mathbf{q}, 0)$ and $G(\mathbf{q}, \infty)$ known from PIMC simulation
- ▶ Other exact properties of G can be incorporated

Dynamic structure factor of the UEG:
($\theta = 1$, $r_s = 10$, $N = 33$, $q = 0.63q_F$)



Incorporating additional information on $S(\mathbf{q}, \omega)$ via dielectric formulation

- ▶ Fluctuation-dissipation theorem:

$$S(\mathbf{q}, \omega) = -\frac{\text{Im} \chi(\mathbf{q}, \omega)}{}$$

- ▶ Exact dynamic spectra not in agreement with exact properties of $G(\mathbf{q}, \omega)$
→ to be discarded as unphysical

$$\chi(\mathbf{q}, \omega) = \frac{1}{1 - v_q [1 - G(\mathbf{q}, \omega)] \chi_0(\mathbf{q}, \omega)}$$

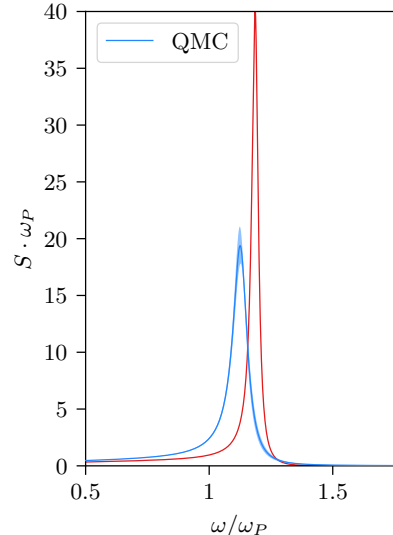
- ▶ Random phase approximation (RPA): $G \equiv 0$

Stochastic sampling of $G(\mathbf{q}, \omega)$ accurately determines $S(\mathbf{q}, \omega)$

Advantages:

- ▶ Limits $G(\mathbf{q}, 0)$ and $G(\mathbf{q}, \infty)$ known from PIMC simulation
- ▶ Other exact properties of G can be incorporated

Dynamic structure factor of the UEG:
($\theta = 1$, $r_s = 10$, $N = 33$, $q = 0.63q_F$)

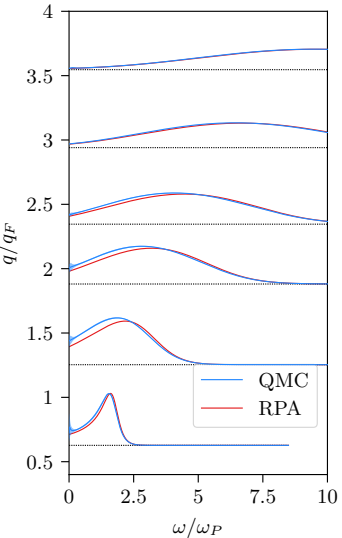


Correlation effects in the dispersion relation: $\theta = 1$, $r_s = 2$

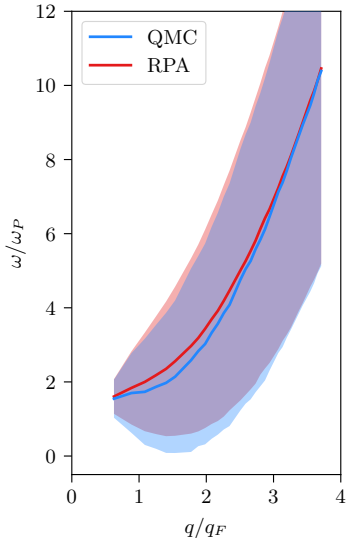
T. Dornheim, S. Groth, J. Vorberger, and M. Bonitz, *Phys. Rev. Lett.* **121**, 255001 (2018)

- ▶ Slight **correlation induced redshift** for intermediate q (at small r_s)

Dynamic structure factor of the UEG:



Peak position and FWHM:

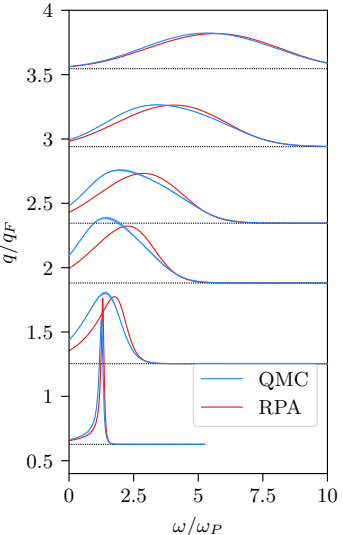


Correlation effects in the dispersion relation: $\theta = 1$, $r_s = 6$

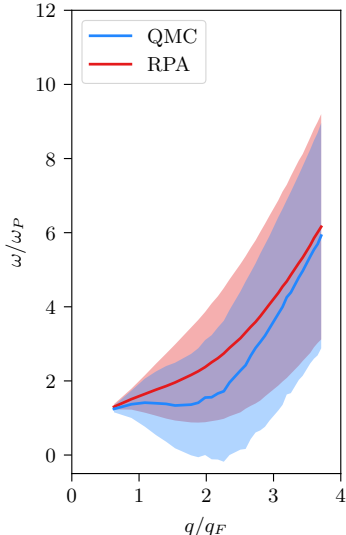
T. Dornheim, S. Groth, J. Vorberger, and M. Bonitz, *Phys. Rev. Lett.* **121**, 255001 (2018)

- ▶ Slight **correlation induced redshift** for intermediate q (at small r_s)
- ▶ **Pronounced redshift and broadening** with increasing r_s

Dynamic structure factor of the UEG:



Peak position and FWHM:

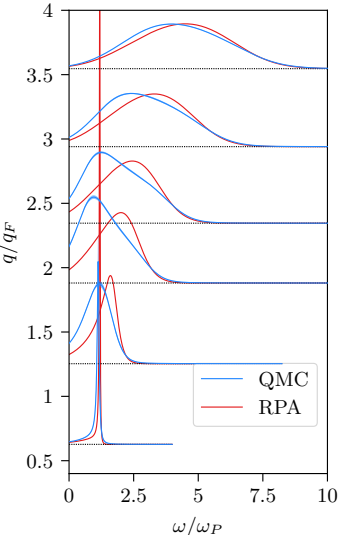


Correlation effects in the dispersion relation: $\theta = 1$, $r_s = 10$

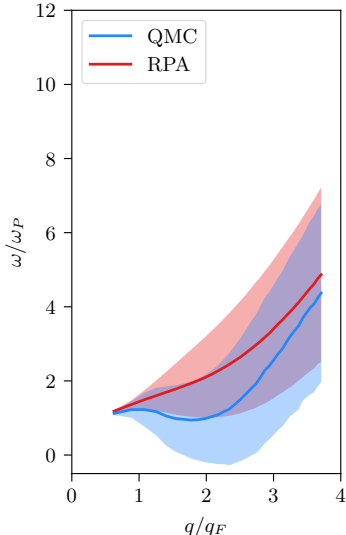
T. Dornheim, S. Groth, J. Vorberger, and M. Bonitz, *Phys. Rev. Lett.* **121**, 255001 (2018)

- ▶ Slight **correlation induced redshift** for intermediate q (at small r_s)
- ▶ **Pronounced redshift and broadening** with increasing r_s
- ▶ **Negative plasmon dispersion** for large r_s around $q = 2q_F$
predicted for dense hydrogen

Dynamic structure factor of the UEG:



Peak position and FWHM:

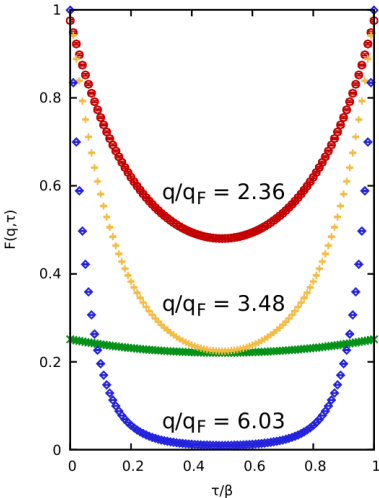


The Static Local Field Correction: *Ab initio* PIMC Simulations

- ▶ PIMC gives direct access to imaginary-time density–density correlation function:

$$F(\mathbf{q}, \tau) = \frac{1}{N} \langle \rho(\mathbf{q}, \tau) \rho(-\mathbf{q}, 0) \rangle$$

Source: S. Groth, **TD**, and J. Vorberger,
Phys. Rev. B **99**, 235122 (2019)



The Static Local Field Correction: *Ab initio* PIMC Simulations

- ▶ PIMC gives direct access to imaginary-time density–density correlation function:

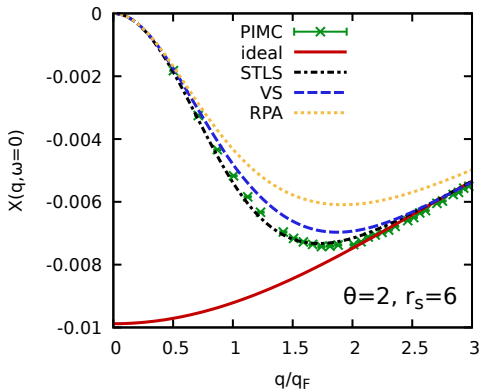
$$F(\mathbf{q}, \tau) = \frac{1}{N} \langle \rho(\mathbf{q}, \tau) \rho(-\mathbf{q}, 0) \rangle$$

- ▶ $F(\mathbf{q}, \tau)$ is directly connected to **static** density response $\chi(\mathbf{q}) = \chi(\mathbf{q}, \omega = 0)$:

$$\chi(\mathbf{q}) = -n \int_0^{\beta} d\tau F(\mathbf{q}, \tau)$$

→ Full \mathbf{q} -dependence from a single simulation of the **unperturbed UEG**

Source: S. Groth, TD, and J. Vorberger,
Phys. Rev. B **99**, 235122 (2019)



The Static Local Field Correction: *Ab initio* PIMC Simulations

- ▶ PIMC gives direct access to imaginary-time density–density correlation function:

$$F(\mathbf{q}, \tau) = \frac{1}{N} \langle \rho(\mathbf{q}, \tau) \rho(-\mathbf{q}, 0) \rangle$$

- ▶ $F(\mathbf{q}, \tau)$ is directly connected to **static** density response $\chi(\mathbf{q}) = \chi(\mathbf{q}, \omega = 0)$:

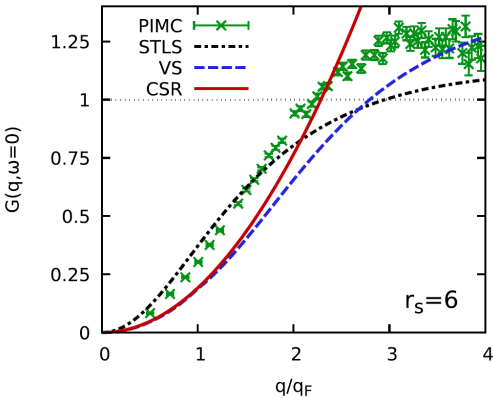
$$\chi(\mathbf{q}) = -n \int_0^{\beta} d\tau F(\mathbf{q}, \tau)$$

→ Full \mathbf{q} -dependence from a single simulation of the **unperturbed UEG**

- ▶ $G(q)$ can be obtained as the deviation from $\chi_0(q)$:

$$G(\mathbf{q}) = 1 - \frac{1}{v_q} \left(\frac{1}{\chi_0(\mathbf{q}, 0)} - \frac{1}{\chi(\mathbf{q})} \right) .$$

Source: S. Groth, TD, and J. Vorberger,
Phys. Rev. B **99**, 235122 (2019)

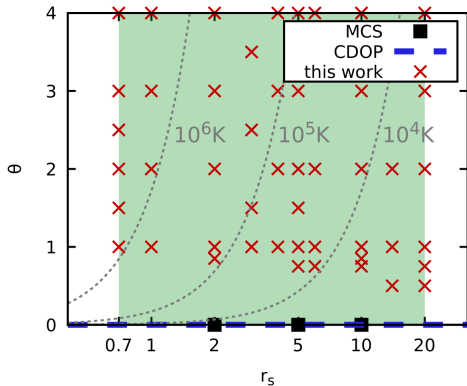


The Static Local Field Correction: Neural-net representation

Extensive set of new PIMC data

- QMC data available at discrete grid ($q; \theta, r_s$)

Source: T. Dornheim *et al.*,
J. Chem. Phys. (2019)

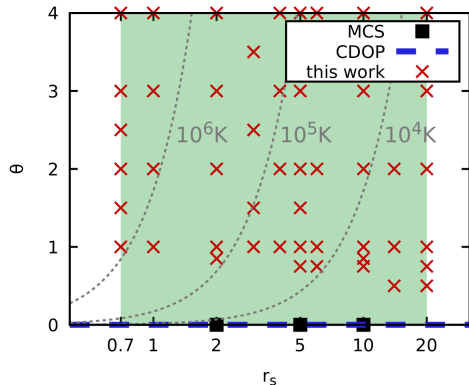


The Static Local Field Correction: Neural-net representation

Extensive set of new PIMC data

- ▶ QMC data available at discrete grid ($q; \theta, r_s$)
- ▶ **Problem:** Applications (DFT, hydrodynamics, . . .) typically require continuous representation

Source: T. Dornheim *et al.*,
J. Chem. Phys. (2019)

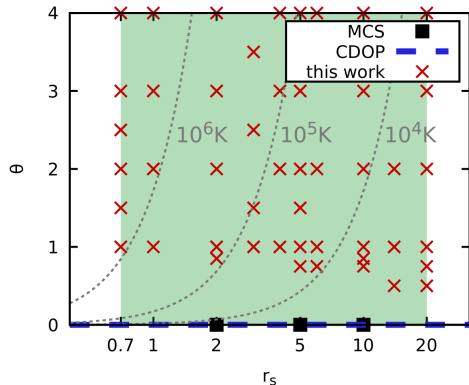


The Static Local Field Correction: Neural-net representation

Extensive set of new PIMC data

- ▶ QMC data available at discrete grid ($q; \theta, r_s$)
- ▶ **Problem:** Applications (DFT, hydrodynamics, . . .) typically require continuous representation
- ▶ Complicated, non-trivial behavior of $G(q; r_s, \theta)$, only few analytical limits are known

Source: T. Dornheim *et al.*,
J. Chem. Phys. (2019)

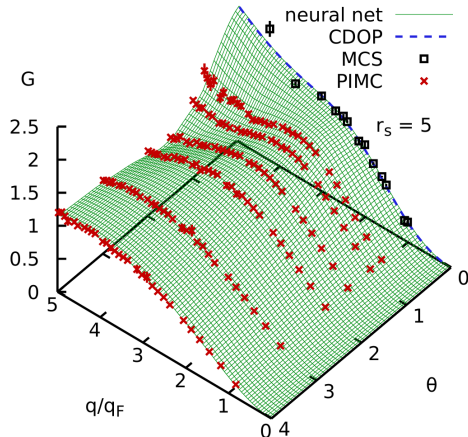


The Static Local Field Correction: Neural-net representation

Extensive set of new PIMC data

- ▶ QMC data available at discrete grid ($q; \theta, r_s$)
- ▶ **Problem:** Applications (DFT, hydrodynamics, . . .) typically require continuous representation
- ▶ Complicated, non-trivial behavior of $G(q; r_s, \theta)$, only few analytical limits are known
- ▶ **Solution:** Neural net as flexible function approximator

Source: T. Dornheim *et al.*,
J. Chem. Phys. (2019)

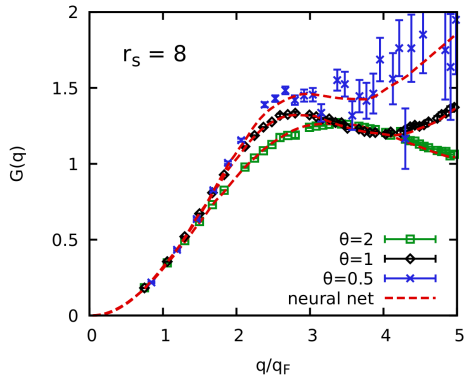


The Static Local Field Correction: Neural-net representation

Extensive set of new PIMC data

- ▶ QMC data available at discrete grid ($q; \theta, r_s$)
- ▶ **Problem:** Applications (DFT, hydrodynamics, . . .) typically require continuous representation
- ▶ Complicated, non-trivial behavior of $G(q; r_s, \theta)$, only few analytical limits are known
- ▶ **Solution:** Neural net as flexible function approximator
- ▶ **Successful validation against independent data!**
- ▶ **Basis for transport quantities, screened ion potential**
Benchmarks for models and simulations

Source: T. Dornheim *et al.*,
J. Chem. Phys. (2019)



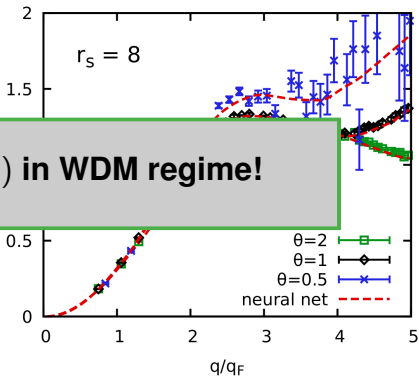
The Static Local Field Correction: Neural-net representation

Extensive set of new PIMC data

- ▶ QMC data available at discrete grid ($q; \theta, r_s$)
- ▶ Problem: Applications (DFT, hydrodynamics) typically require
- ▶ Comp. analytic
- ▶ Solution: Neural net as flexible function approximator
- ▶ **Successful validation against independent data!**
- ▶ Basis for transport quantities, screened ion potential
Benchmarks for models and simulations

Source: T. Dornheim *et al.*,
J. Chem. Phys. (2019)

Complete *ab initio* data for $G(q; r_s, \theta)$ in WDM regime!



Part II: Warm dense matter out of equilibrium

- ▶ **increasing experimental relevance:**

femtosecond pump-probe experiments with lasers and free electron lasers:
XFEL (Hamburg), LCLS (Stanford), China
e.g. A. Ng, S. Glenzer

- ▶ **Theoretical approaches**

1. Quantum kinetic theory⁴, nonequilibrium Green functions⁵: Gericke *et al.*, Vorberger *et al.*, Bornath *et al.*
new simulations currently being developed in Kiel (WDM conference 2019)
2. Time-dependent DFT (TD-DFT), e.g. A. Baczeswki *et al.*
3. (Quantum) Hydrodynamics

⁴M. Bonitz, "Quantum Kinetic Theory", 2nd ed., Springer 2016

⁵D. Kremp *et al.*, "Quantum Statistics of Nonideal Plasmas", Springer 2005

Nonequilibrium Green functions approach to the dynamical structure factor

VOLUME 84, NUMBER 8

PHYSICAL REVIEW LETTERS

21 FEBRUARY 2000

Real-Time Kadanoff-Baym Approach to Plasma Oscillations in a Correlated Electron Gas

N.-H. Kwong* and M. Bonitz

Fachbereich Physik, Universität Rostock, Universitätsplatz 3, D-18051 Rostock, Germany
(Received 30 August 1999)

A nonequilibrium Green's functions approach to the collective response of correlated Coulomb systems at finite temperatures is presented. It is shown that solving Kadanoff-Baym-type equations of motion for the two-time correlation functions including the external perturbing field allows one to compute the plasmon spectrum with collision effects in a systematic and consistent way. The scheme has a "built-in" sum-rule preservation and is simpler to implement numerically than the equivalent equilibrium approach based on the Bethe-Salpeter equation.

PACS numbers: 73.20.Mf, 05.30.-d

- ▶ Relation to equilibrium approaches: M. Bonitz, "Quantum Kinetic Theory", 2nd ed., Springer (2016)
- ▶ Similar approach in TD-DFT (Bertsch, Yabana 1995)

Nonequilibrium Green functions approach to the dynamical structure factor

VOLUME 84, NUMBER 8

PHYSICAL REVIEW LETTERS

21 FEBRUARY 2000

Real-Time Kadanoff-Baym Approach to Plasma Oscillations in a Correlated Electron Gas

N.-H. Kwong* and M. Bonitz

Fachbereich Physik, Universität Rostock, Universitätsplatz 3, D-18051 Rostock, Germany
(Received 30 August 1999)

A nonequilibrium Green's functions approach to the collective response of correlated Coulomb systems at finite temperatures is presented. It is shown that solving Kadanoff-Baym-type equations of motion for the two-time correlation functions including the external perturbing field allows one to compute the plasmon spectrum with collision effects in a systematic and consistent way. The scheme has a "built-in" sum-rule preservation and is simpler to implement numerically than the equivalent equilibrium approach based on the Bethe-Salpeter equation.

PACS numbers: 73.20.Mf, 05.30.-d

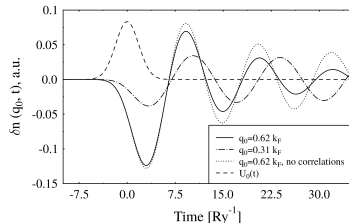


FIG. 1. Density fluctuation of a strongly correlated electron gas for two wave numbers. For comparison, the uncorrelated response for one wave number (dotted line) and the exciting field (dashes) are shown, too. k_F denotes the Fermi momentum, $Ry = 13.6$ eV.

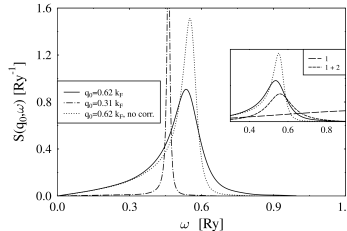


FIG. 2. Dynamic structure factor (12) for the correlated electron gas of Fig. 1 (same line styles). Inset shows S for $q_0 = 0.62k_F$ and contains two other approximations to the correlations corresponding to retaining the first diagram in Eq. (17) and first plus second diagrams, respectively.

Quantum hydrodynamics (QHD) for plasmas: problems and open questions

- ▶ **Examples of quantum fluid theories**
 - ▶ Fermi liquid theory (Landau, Abrikosov...): metals, quasiparticles non-Fermi liquids (Luttinger)
 - ▶ quantum spin liquids (magnetic materials); superfluid theory (Bogolyubov)
- ▶ **Kinetic theory approach:** moments of the momentum distribution function:
 $n \sim \langle v^0 \rangle, \quad \mathbf{u} \sim \langle \mathbf{v}^1 \rangle, \quad P \sim \langle \mathbf{v}\mathbf{v} \rangle$ etc. \Rightarrow hierarchy of moment equations
 - ▶ a) truncation of the moment hierarchy (phenomenological closure)
 - ▶ b) asymptotic schemes, small parameter, e.g. $\epsilon = \lambda_{\text{mfp}}/L \ll 1$,
 $f(\mathbf{r}, \mathbf{v}, t) = f_0(\mathbf{r}, \mathbf{v}, t) + \epsilon f_1(\mathbf{r}, \mathbf{v}, t) + \dots$
$$f_0(\mathbf{r}, \mathbf{v}, t) = n(\mathbf{r}, t) \left(\frac{m}{2\pi k_B T(\mathbf{r}, t)} \right)^{3/2} \exp \left[\frac{m(\mathbf{v} - \mathbf{u}(\mathbf{r}, t))^2}{2k_B T(\mathbf{r}, t)} \right],$$

 f_0 : collision integrals vanish \Rightarrow no heat flux, no viscous stress
 f_1 expanded into Laguerre/Sonine polynomials (Chapman-Enskog)
- ▶ **no similar mature approaches to quantum plasmas**, except for linear response theory (Zubarev, Röpke, ... generalized Gibbs ensemble)

QHD for plasmas: problems and open questions

Quantum hydrodynamics – status:

- ▶ straightforward for a single particle and for bosons
- ▶ fermions, plasmas: questionable assumptions in derivation^a
- ▶ In many papers: incorrect coefficients in QHD equations^b

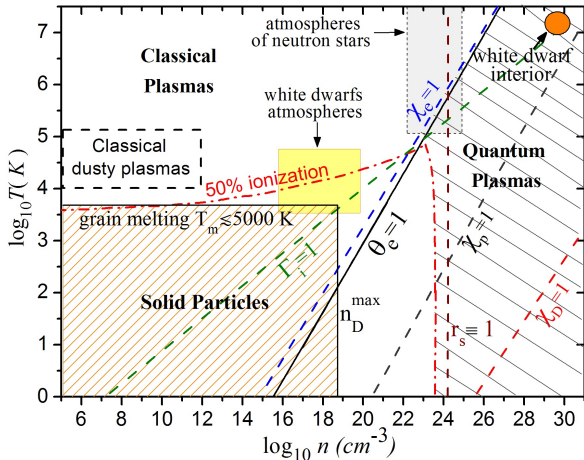
questionable predictions:

- ▶ “novel attractive forces” between ions in quantum plasmas^c
- ▶ “spinning quantum plasmas”,
- ▶ most recent example: “quantum dusty plasmas” (see figure)^d

questionable claims of relevance:

- ▶ semiconductors, metals
- ▶ white dwarfs, magnetars, neutron stars

Are they sure?? Can they prove it??
how important are solitons in neutron starts??



^aManfredi, Haas, PRB 2001

^bclarification: Michta, Graziani, Bonitz, Contrib. Plasma Phys. **55**, 437 (2015),
Moldabekov *et al.*, Phys. Plasmas **25**, 031903 (2018), open access

^cShukla, Eliasson, PRL **108**, 165007 (2012); correction: Bonitz *et al.*, PRE **87**, 033105 (2013), Moldabekov *et al.*, Phys. Plasmas (2015)

^dShukla, Ali, Phys. Plasmas **12**, 114502 (2005);

clarification: Bonitz, Moldabekov, Ramazanov, Phys. Plasmas **26**, 090601 (2019), perspectives article, Editors' pick, open access

Contributions to Plasma Physics

CPP

enforce high quality standards: manuscripts should⁶

1. present an important **advance to plasma physics**;
2. contain a **convincing motivation** of the research in the introduction explaining the importance of the work;
3. present **applications to concrete plasmas** (in case of experiments) and—in case of theory—**clear predictions for real plasmas**, including their physical parameters;
4. not be purely formal studies of mathematical properties of equations, for example, in terms of dimensionless parameters, without application to real plasmas, as discussed in 3.

⁶M. Bonitz, Editorial: Contrib. Plasma Phys. **59** (1), 8 (2019)

Fluid description of quantum dynamics

- ▶ N interacting identical quantum particles, hamiltonian

$$\hat{H} = \sum_{i=1}^N \left(-\frac{\hbar^2}{2m} \nabla_i^2 + V(\mathbf{r}_i) \right) + \frac{1}{2} \sum_{i \neq j} w_{ij}(\mathbf{R}),$$

$\mathbf{R} = (\mathbf{r}_1, \sigma_1; \mathbf{r}_2, \sigma_2; \dots \mathbf{r}_N, \sigma_N)$, \mathbf{r}_i are the particle coordinates and σ_i their spin projections.

- ▶ for a pure state: dynamics governed by the **N-particle Schrödinger equation**

$$i\hbar \frac{\partial \Psi(\mathbf{R}, t)}{\partial t} = \hat{H}\Psi(\mathbf{R}, t), \quad \Psi(\mathbf{R}, t_0) = \Psi_0(\mathbf{R}),$$

normalization: $\sum_{\sigma_1 \dots \sigma_N} \int d^{3N}R |\Psi(\mathbf{R}, t)|^2 = N$,

for particles with spin s : $g_s = 2s + 1$ different spin projections

- ▶ ansatz with **real amplitude and phase** (Bohm, Madelung)⁷:

$$\Psi(\mathbf{R}, t) = A(\mathbf{R}, t) e^{\frac{i}{\hbar} S(\mathbf{R}, t)}, \quad A, S \in \mathcal{R}.$$

- ▶ can be used for semiclassical molecular dynamics, e.g. Gericke, Gregori *et al.* (2018)

⁷E. Madelung, Z. Phys. (1927), D. Bohm, Phys. Rev. (1952)

Quantum hydrodynamics for 1 particle

hydrodynamic fields from wave function (for pure state):

$$n(\mathbf{r}, t) = A^2(\mathbf{r}, t), \quad \text{density,}$$
$$\mathbf{p}(\mathbf{r}, t) = m\mathbf{v}(\mathbf{r}, t) = \nabla S(\mathbf{r}, t), \quad \text{momentum,}$$

exact “hydrodynamic” equations:

$$\frac{\partial n}{\partial t} + \nabla(\mathbf{v}n) = 0,$$
$$\frac{\partial \mathbf{p}}{\partial t} + \mathbf{v}\nabla \mathbf{p} = -\nabla(V + Q),$$
$$Q[n(\mathbf{r}, t)] = -\frac{\hbar^2}{2m} \frac{\nabla^2 n^{1/2}}{n^{1/2}}, \quad \text{“Bohm potential”,}$$

Modifications for N fermions:

- ▶ spin statistics (Pauli principle): N different orbitals $\phi_i \Rightarrow$ different n_i, \mathbf{p}_i
- ▶ interaction w_{ij} between particles
- ▶ statistical weight f_i of each orbital?
- ▶ coupling of orbitals? Definition of mean n and \mathbf{p} ?

Statistical description of N-particle quantum system⁸

- mixed state described by **N-particle density operator**:

$$\hat{\rho}(t) = \sum_a p_a |\Psi^a(t)\rangle\langle\Psi^a(t)|, \quad \text{Tr } \hat{\rho}(t) = 1,$$

sum over projection operators on all solutions of the Schrödinger equation,

p_a : real probabilities, $0 \leq p_a \leq 1$, with $\sum_a p_a = 1$

- **one-particle reduced density operator**:

$$\hat{F}_1(t) \equiv N \text{Tr}_{2\dots N} \hat{\rho}(t), \quad \text{Tr}_1 \hat{F}_1 = N.$$

- equation of F_1 : **quantum kinetic equation**, $\hat{F}_{12} = \hat{F}_1 \hat{F}_2 + \hat{g}_{12}$:

$$i\hbar \frac{\partial \hat{F}_1}{\partial t} - [\hat{H}_1, \hat{F}_1] = \text{Tr}_2 [\hat{w}_{12}, \hat{g}_{12}] \equiv \hat{l}_1 [\hat{g}_{12}], \quad \text{collision integral ,}$$

$$\hat{H}_1(t) = \hat{H}_1 + \hat{H}_1^H(t), \quad \hat{H}_1^H(t) \equiv \text{Tr}_2 \hat{w}_{12} \hat{F}_2(t), \quad \text{mean field ,}$$

⁸M. Bonitz, "Quantum Kinetic Theory", 2nd ed., Springer 2016

Density matrix equation in Hartree approximation

- ▶ **mean field approximation** (no anti-symmetrization, no correlations):

$$\Psi(\mathbf{R}, t) \approx \phi_{\alpha_1}(\mathbf{r}_1) \cdot \phi_{\alpha_2}(\mathbf{r}_2) \cdots \phi_{\alpha_N}(\mathbf{r}_N), \quad \langle \phi_\alpha | \phi_\beta \rangle = \delta_{\alpha, \beta}$$

$\phi_{\alpha_k}(\mathbf{r}_k)$: single-particle orbital occupied by particle k ,

for density operators: no antisymmetrization and $\hat{l}_1 = 0 \Rightarrow \hat{F}_{12} \approx \hat{F}_1 \hat{F}_2$

- ▶ **coordinate representation:** $\langle \mathbf{r}' | \hat{F}_1(t) | \mathbf{r}'' \rangle = f(\mathbf{r}', \mathbf{r}'', t)$, density matrix

$$\begin{aligned} i\hbar \frac{\partial}{\partial t} f(\mathbf{r}', \mathbf{r}'', t) &= -\frac{\hbar^2}{2m} \left(\nabla_{\mathbf{r}'}^2 - \nabla_{\mathbf{r}''}^2 \right) f(\mathbf{r}', \mathbf{r}'', t) \\ &\quad + \left\{ U^{\text{eff}}(\mathbf{r}', t) - U^{\text{eff}}(\mathbf{r}'', t) \right\} f(\mathbf{r}', \mathbf{r}'', t) \end{aligned}$$

$$U^{\text{eff}}(\mathbf{r}, t) = V(\mathbf{r}, t) + U^{\text{H}}(\mathbf{r}, t),$$

$$U^{\text{H}}(\mathbf{r}, t) = g_s \int d\bar{\mathbf{r}} w(r - \bar{r}) f(\bar{r}, \bar{r}, t),$$

diagonal element of the density matrix: $f(\mathbf{r}, \mathbf{r}, t) = n(\mathbf{r}, t)$, density

Hartree approximation for fermions

- ▶ **mean field approximation** (no anti-symmetrization, no correlations):

$$\Psi(\mathbf{R}, t) \approx \phi_{\alpha_1}(\mathbf{r}_1) \cdot \phi_{\alpha_2}(\mathbf{r}_2) \cdots \phi_{\alpha_N}(\mathbf{r}_N), \quad \langle \phi_{\alpha} | \phi_{\beta} \rangle = \delta_{\alpha, \beta}$$

Thermodynamic equilibrium: orbitals $\phi_1, \phi_2 \dots$ occupied with probability $f_i = [e^{\beta(\epsilon_i - \mu)} + 1]^{-1}$, $i = 1 \dots \infty$

- ▶ One-particle density operator and density matrix:

$$\hat{F}_1 = N \text{Tr}_{2\dots N} \sum_{\alpha} \frac{1}{Z_G} e^{-\beta(E_{\alpha} - \mu N_{\alpha})} |\psi_{\alpha}\rangle \langle \psi_{\alpha}| = N \sum_{i=1}^{\infty} f_i |\phi_i\rangle \langle \phi_i|$$

$$f(\mathbf{r}', \mathbf{r}'', t) = N \sum_{i=1}^{\infty} f_i \phi_i(\mathbf{r}', t) \phi_i^*(\mathbf{r}'', t),$$

- ▶ Equation for f solved by set of nonlinear "Hartree-"Schrödinger (t-dependent Kohn-Sham) equations:

$$i\hbar \frac{\partial}{\partial t} \phi_i(\mathbf{r}, t) = \left\{ -\frac{\hbar^2}{2m} \nabla_{\mathbf{r}}^2 + V(\mathbf{r}, t) + U_F^H(\mathbf{r}, t) \right\} \phi_i(\mathbf{r}, t),$$

$$U_F^H[n(\mathbf{r}, t)] = \int d\mathbf{r}_2 w(\mathbf{r} - \mathbf{r}_2) [g_s n(\mathbf{r}_2, t) - n_0],$$

U_F^H : Hartree mean field, $n(\mathbf{r}, t) = \sum_{i=1}^{\infty} f_i |\phi_i(\mathbf{r}, t)|^2$. n_0 : background

Microscopic QHD equations (MQHD)¹⁰

- ▶ in TDSE: introduce real amplitude ($A_i = n_i^{1/2}$) and phase for each orbital:
- ▶ restore exchange-correlation effects formally exactly⁹: either
 - i) potential $V^{\text{xc}} = V^{\text{xc}}[n(\mathbf{r}, \tilde{t})]$, from TD-DFT, or, alternatively,
 - ii) collision integral $I_i[g_{12}(\tilde{t})]$ from quantum kinetic theory

$$\begin{aligned}\frac{\partial n_i}{\partial t} + \nabla(\mathbf{v}_i n_i) &= 0, \\ \frac{\partial \mathbf{p}_i}{\partial t} + \mathbf{v}_i \text{div} \mathbf{p}_i &= -\nabla(V(\mathbf{r}, t) + U^H + Q_i + V^{\text{xc}} + I_i), \\ U^H[n(\mathbf{r}, t)] &= \int d\mathbf{r}_2 w(\mathbf{r} - \mathbf{r}_2)[g_s n(\mathbf{r}_2, t) - n_0], \\ Q_i(\mathbf{r}, t) &= -\frac{\hbar^2}{2m} \frac{\nabla^2 \sqrt{n_i(\mathbf{r}, t)}}{\sqrt{n_i(\mathbf{r}, t)}}.\end{aligned}$$

- ▶ $n(\mathbf{r}, t) = \sum_{i=1}^{\infty} f_i \cdot |\phi_i(\mathbf{r}, t)|^2$, f_i statistical weight (Fermi function), $g_s = 2s + 1$.
- ▶ ⇒ exact formulation of the many-body problem (with proper set of orbitals), equivalent to TD-DFT

⁹in general: memory effects (non-adiabatic), i.e. $t_0 \leq \tilde{t} \leq t$

¹⁰Bonitz *et al.*, Phys. Plasmas **26**, 090601 (2019), agrees with Manfredi, Fields Inst. Comm. 2005

Derivation of QHD equations from MQHD¹¹

- ▶ consider mean field (Hartree / quantum Vlasov) approximation: $V^{\text{xc}} \equiv I_i \equiv 0$
- ▶ average MQHD equations over i with weights f_i
- ▶ define hydrodynamic (average) quantities:

$$\bar{n}(\mathbf{r}, t) = \frac{1}{N} \sum_{i=1}^{\infty} f_i n_i(\mathbf{r}, t),$$

$$\bar{\mathbf{p}}(\mathbf{r}, t) = \frac{1}{N} \sum_{i=1}^{\infty} f_i \mathbf{p}_i(\mathbf{r}, t),$$

$$\bar{Q}(\mathbf{r}, t) = -\frac{\hbar^2}{2mN} \sum_{i=1}^{\infty} f_i \frac{\nabla^2 \sqrt{n_i(\mathbf{r})}}{\sqrt{n_i(\mathbf{r})}} \neq \frac{\hbar^2}{2mN} \frac{\nabla^2 \sqrt{\bar{n}(\mathbf{r})}}{\sqrt{\bar{n}(\mathbf{r})}} \equiv Q_1[\bar{n}].$$

- ▶ final equality was *postulated* by Manfredi and Haas (PRB 2001, Fields Inst. Comm. 2005) reproducing *single-particle* QHD equations (with Hartree potential)
- ▶ When does it hold? What are the corrections? ⇒ perform strict derivation

¹¹Bonitz *et al.*, Phys. Plasmas 2019

Derivation of QHD equations (contd.)¹²

- ▶ use average of product: $\overline{a_i b_i} = \bar{a} \cdot \bar{b} + \overline{\delta a_i \delta b_i}$,
- ▶ result: **formally exact QHD equations** from orbital average of MQHD (TD-DFT):

$$\frac{\partial \bar{n}}{\partial t} + \frac{1}{m} \nabla (\bar{\mathbf{p}} \cdot \bar{n}) = J_{np}^{\Delta}$$

$$\frac{\partial \bar{\mathbf{p}}}{\partial t} + \frac{1}{m} \bar{\mathbf{p}} \cdot \operatorname{div} \bar{\mathbf{p}} = -\nabla \left(V(\mathbf{r}, t) + U_F^H[\bar{n}] + Q_1[\bar{n}] + Q^{\Delta} + V^{xc}[\bar{n}] \right) + J_{pp}^{\Delta}$$

- ▶ three correction terms (correlation functions):

$$J_{np}^{\Delta} = -\frac{1}{m} \nabla \overline{\delta \mathbf{p}_i \delta n_i}, \quad Q^{\Delta} \approx \frac{\hbar^2}{2m\bar{n}} \overline{\delta A_i \cdot \nabla^2 \delta A_i} + O\left(\left(\frac{\delta A_i}{A}\right)^2\right),$$

$$J_{pp}^{\Delta} = -\frac{1}{m} \overline{\delta \mathbf{p}_i \operatorname{div} \delta \mathbf{p}_i} = \frac{1}{\bar{n}} \partial_{\beta} \bar{P}_{\alpha\beta} = \frac{1}{\bar{n}} \nabla \bar{P}_F + \frac{1}{\bar{n}} \partial_{\gamma} \bar{\sigma}_{\alpha\gamma}, \quad \gamma \neq \alpha, \quad \bar{\sigma} : \text{stress tensor},$$

- ▶ special case: **ideal Fermi gas** of dimension $D = 1, 2, 3$, $T = 0$: $\bar{\sigma}_{\alpha\gamma} \rightarrow 0$ and

$$J_{pp}^{\Delta} = \frac{1}{D} \nabla \overline{\delta E_{\text{kin}}} = \frac{m}{2(D+2)} \nabla v_F^2 = \frac{1}{2\bar{n}} \nabla \bar{P}^{\text{id}}.$$

¹²Bonitz *et al.*, Phys. Plasmas 2019

Test case plasma oscillations: linearization of MQHD-equations¹³

- stability conditions without excitation:

$$\begin{aligned}\partial_t n_{i0} &= \partial_t \mathbf{p}_{i0} = \bar{\mathbf{v}}_{i0} = 0 \\ \mathbf{v}_{i0} \operatorname{div} \mathbf{p}_{i0} &= -\nabla(U_0^H + Q_{i0})\end{aligned}$$

- monochromatic weak excitation: $V_1^{\text{ext}}(\mathbf{r}, t) = \tilde{V}_1^{\text{ext}} e^{-i\hat{\omega}t+i\mathbf{qr}}$, where $\hat{\omega} = \omega + i\epsilon$, $\epsilon > 0$
- linearization and Fourier-Laplace transform:

$$\begin{aligned}n_{i0} &\rightarrow n_{i0} + n_{i1}; \mathbf{v}_{i0} \rightarrow \mathbf{v}_{i0} + \mathbf{v}_{i1}; \\ U_0^H &\rightarrow U_0^H + U_1^H; Q_{i0} \rightarrow Q_{i0} + Q_{i1}, \quad U_1^{\text{eff}} = V_1^{\text{ext}} + U_1^H\end{aligned}$$

- density response exactly coincides with random phase approximation (RPA)

$$\begin{aligned}\tilde{n}_1(\mathbf{q}, \hat{\omega}) &= \frac{1}{N} \sum_{i=1}^{\infty} f_i \tilde{n}_{i1}(\mathbf{q}, \hat{\omega}) = \tilde{U}_1^{\text{eff}}(\mathbf{q}, \hat{\omega}) \tilde{\Pi}_1^R(\mathbf{q}, \hat{\omega}) \\ \tilde{\Pi}_1^R(\mathbf{q}, \hat{\omega}) &= \frac{1}{N} \sum_{i=1}^{\infty} \frac{f_i}{(\hat{\omega} - \mathbf{q} \cdot \mathbf{v}_{i0})^2 - \frac{\hbar^2 q^4}{4m^2}}.\end{aligned}$$

¹³Bonitz *et al.*, Phys. Plasmas 2019, result agrees with Manfredi, Fields Inst. Comm. 2005

Test case plasma oscillations: linearization of QHD equations¹⁵

- ▶ Hartree approximation, neglect correlation terms
- ▶ linearization and Fourier-Laplace transform:

$$\bar{n}_0 \rightarrow \bar{n}_0 + \bar{n}_1; \bar{\mathbf{v}}_0 \rightarrow \bar{\mathbf{v}}_0 + \bar{\mathbf{v}}_1; U_0^H \rightarrow U_0^H + U_1^H;$$

$$Q[\bar{n}] \rightarrow -\frac{\hbar^2}{2m} \frac{\nabla^2 \sqrt{\bar{n}_0}}{\sqrt{\bar{n}_0}} + \frac{\hbar^2}{4m} \nabla^2 \sqrt{\bar{n}_1},$$

$$\bar{P}_0^{\text{id}} \rightarrow \frac{2}{D+2} \bar{n}_0 E_F(\bar{n}_0) + \frac{2}{D} \frac{\bar{n}_1}{\bar{n}_0} E_F(\bar{n}_0),$$

- ▶ plasmon dispersion – QHD vs. MQHD (RPA): agreement only in 1D, for $\omega \geq \omega_{pl}$

$$\omega_{\text{QHD}}^2(q) = \omega_{pl}^2 + \frac{1}{D} v_F^2 q^2 + \frac{\hbar^2}{4m^2} q^4,$$

$$\omega_{\text{MQHD}}^2(q) = \omega_{pl}^2 + \frac{3}{D+2} v_F^2 q^2 + (1 - \delta_{2,D}) \frac{\hbar^2}{4m^2} q^4,$$

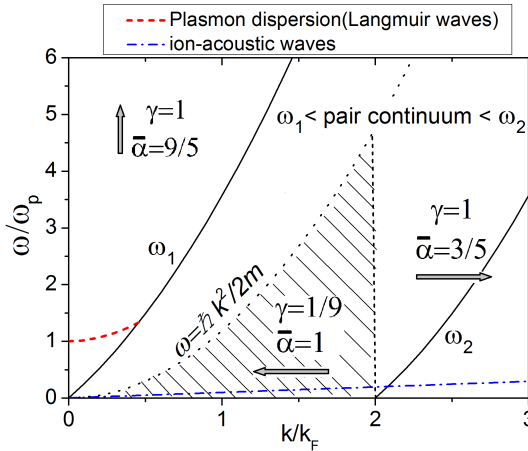
- ▶ for $\omega < \omega_{pl}$: Bohm potential Q is factor 9 too big \Rightarrow incorrect acoustic modes and statically screened potential¹⁴

¹⁴ Michta *et al.*, CPP **55**, 437 (2015), Moldabekov *et al.*, Phys. Plasmas **25**, 031903 (2018)

¹⁵ Bonitz *et al.*, Phys. Plasmas **26**, 090601 (2019)

Correction of coefficients in QHD equations¹⁶

- Comparison to RPA reveals ω - and k -dependence of pressure ($\bar{\alpha}$) and Bohm potential (γ).
In addition: dependence on temperature, dimensionality



¹⁶Figure for 3D case, $T = 0$, from: Moldabekov, Bonitz, and Ramazanov, Phys. Plasmas **25**, 031903 (2018)

Summary

- ▶ *ab initio* QMC simulations provide complete thermodynamic data for warm dense uniform electron gas¹⁷
- ▶ accurate functional $f_{xc}(r_s, \Theta, \xi)$ input for finite-T LDA-DFT, implemented in [Libxc](#) (LDA_XC_GDSMFB)
- ▶ ab initio data for inhomogeneous EG¹⁸ ⇒ accurate parametrization of static local field correction¹⁹ $G(q)$
- ▶ first *ab initio* data for the dynamic structure factor $S(q, \omega)$ of warm dense electrons²⁰

¹⁷T. Dornheim *et al.*, Phys. Reports (2018)

¹⁸S. Groth *et al.*, J. Chem. Phys. (2017); T. Dornheim *et al.*, Phys. Rev. E (2017)

¹⁹T. Dornheim *et al.*, J. Chem. Phys. (2019)

²⁰T. Dornheim *et al.*, Phys. Rev. Lett. (2018); S. Groth *et al.*, Phys. Rev. B (2019)

²¹Zh. Moldabekov *et al.*, Phys. Plasmas (2018); M. Bonitz *et al.*, Phys. Plasmas (2019)

²²N. Schlünzen *et al.*, arXiv:1909.11489

Summary

- ▶ *ab initio* QMC simulations provide complete thermodynamic data for warm dense uniform electron gas¹⁷
- ▶ accurate functional $f_{xc}(r_s, \Theta, \xi)$ input for finite-T LDA-DFT, implemented in [Libxc](#) (LDA_XC_GDSMFB)
- ▶ ab initio data for inhomogeneous EG¹⁸ ⇒ accurate parametrization of static local field correction¹⁹ $G(q)$
- ▶ first *ab initio* data for the dynamic structure factor $S(q, \omega)$ of warm dense electrons²⁰
- ▶ **QHD** rigorously derived from Microscopic QHD (TDDFT), coefficients depend on excitation conditions²¹
⇒ systematic improvements possible, promising for large space and time scales in WDM

¹⁷T. Dornheim *et al.*, Phys. Reports (2018)

¹⁸S. Groth *et al.*, J. Chem. Phys. (2017); T. Dornheim *et al.*, Phys. Rev. E (2017)

¹⁹T. Dornheim *et al.*, J. Chem. Phys. (2019)

²⁰T. Dornheim *et al.*, Phys. Rev. Lett. (2018); S. Groth *et al.*, Phys. Rev. B (2019)

²¹Zh. Moldabekov *et al.*, Phys. Plasmas (2018); M. Bonitz *et al.*, Phys. Plasmas (2019)

²²N. Schlünzen *et al.*, arXiv:1909.11489

Summary

- ▶ *ab initio* QMC simulations provide complete thermodynamic data for warm dense uniform electron gas¹⁷
- ▶ accurate functional $f_{xc}(r_s, \Theta, \xi)$ input for finite-T LDA-DFT, implemented in [Libxc](#) (LDA_XC_GDSMFB)
- ▶ ab initio data for inhomogeneous EG¹⁸ ⇒ accurate parametrization of static local field correction¹⁹ $G(q)$
- ▶ first *ab initio* data for the dynamic structure factor $S(q, \omega)$ of warm dense electrons²⁰
- ▶ **QHD** rigorously derived from Microscopic QHD (TDDFT), coefficients depend on excitation conditions²¹
⇒ systematic improvements possible, promising for large space and time scales in WDM
- ▶ Electronic correlations and correlation build up (thermalization, dynamical screening, Auger processes etc.) are captured by (Nonequilibrium) **Green functions**. Highly efficient new computational techniques available²²

¹⁷T. Dornheim *et al.*, Phys. Reports (2018)

¹⁸S. Groth *et al.*, J. Chem. Phys. (2017); T. Dornheim *et al.*, Phys. Rev. E (2017)

¹⁹T. Dornheim *et al.*, J. Chem. Phys. (2019)

²⁰T. Dornheim *et al.*, Phys. Rev. Lett. (2018); S. Groth *et al.*, Phys. Rev. B (2019)

²¹Zh. Moldabekov *et al.*, Phys. Plasmas (2018); M. Bonitz *et al.*, Phys. Plasmas (2019)

²²N. Schlünzen *et al.*, arXiv:1909.11489

Outlook: simulating WDM out of equilibrium—combination of methods promising

- **QHD** derived via averaging over all orbitals $\phi_\alpha(\mathbf{r}) \Rightarrow$ no resolution of microscopic lengths scales, $L_A \sim a_B, \lambda_{TF}$, and associated times \Rightarrow advantage: extendable to large length and time scales

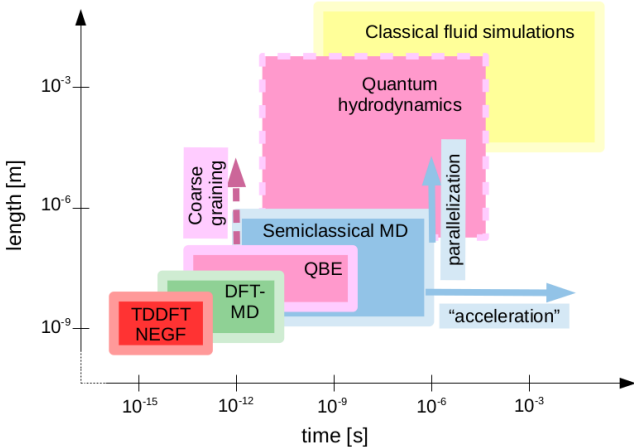


Figure: modified from M. Bonitz et al., *Front. Chem. Science Engin.* (2019); QBE: quantum Boltzmann equation, NEGF: Nonequilibrium Green functions

Outlook: simulating WDM out of equilibrium—combination of methods promising

- ▶ **QHD** derived via averaging over all orbitals $\phi_\alpha(\mathbf{r}) \Rightarrow$ no resolution of microscopic lengths scales, $L_A \sim a_B, \lambda_{TF}$, and associated times \Rightarrow advantage: extendable to large length and time scales
- ▶ **DFT-MD** and **TD-DFT** capture atomic scales and inhomogeneity effects. But: miss electronic correlations (inaccurate band gap, ionization energies, no Auger processes etc.)

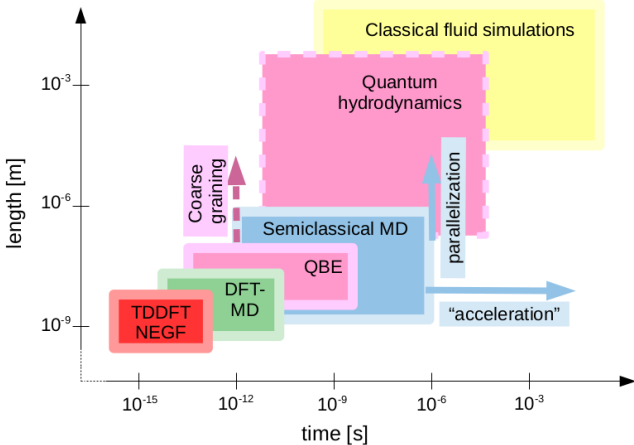


Figure: modified from M. Bonitz et al., *Front. Chem. Science Engin.* (2019); QBE: quantum Boltzmann equation, NEGF: Nonequilibrium Green functions

Outlook: simulating WDM out of equilibrium—combination of methods promising

- ▶ **QHD** derived via averaging over all orbitals $\phi_\alpha(\mathbf{r}) \Rightarrow$ no resolution of microscopic lengths scales, $L_A \sim a_B, \lambda_{TF}$, and associated times \Rightarrow advantage: extendable to large length and time scales
- ▶ **DFT-MD** and **TD-DFT** capture atomic scales and inhomogeneity effects. But: miss electronic correlations (inaccurate band gap, ionization energies, no Auger processes etc.)
- ▶ **Green functions** capture electronic correlations, correlation build up and electron thermalization

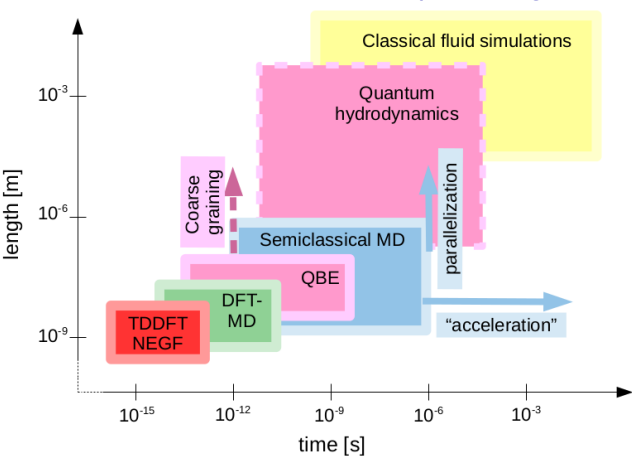


Figure: modified from M. Bonitz et al., *Front. Chem. Science Engin.* (2019); QBE: quantum Boltzmann equation, NEGF: Nonequilibrium Green functions